nature food

Supplementary information

https://doi.org/10.1038/s43016-024-01081-z

Improved alternate wetting and drying irrigation increases global water productivity

Supplementary Information

Supplementary text

1. Potential physiological mechanisms of AWD-induced ΔY
2. Relations between field water depth and soil water potential
3. Calculation of water stress index

Supplementary Tables

1. Comparison of AWD effects on rice yield (ΔY) between this study and previous studies
2. List of variables included in this study
3. Model details for predicting AWD effects on yield
4. Model details for predicting AWD effects on irrigation water use
5. Global Hydrological models used for calculating water stress index (WSI)
6. Summary of physiological processes responsible for AWD effects on rice yield proposed by previous studies
7. Information of experiments used for parameter calibration of the empirical models between field water depth and soil water potential
8. Calibrated parameters from each group of site×year×AWD treatment observations
9. Calibrated model parameters and model performance of the empirical statistical models used to quantify relationships between field water depth and soil water potential based on power and exponential functions
10. Probability distribution of model coefficients and input data for uncertainty estimation
11. List of studies in our database that explicitly recorded experimental conditions of weeds, insects and diseases
12. Prediction of the lowest threshold of soil water potential, priority areas and water productivity improvements over the period of 2001-2015 based on two global soil datasets (Global Soil Dataset and Harmonized World Soil Database)
13. Changes in irrigation water use (ΔIRR) and water productivity (ΔWP) from adopting the soil water potential-based (SWP) and field water depth-based (FWD) AWD scheme, as compared to continuous flooding
14. Results based on different approaches converting field water depth to soil water potential
15. Sensitivity tests against rice cultivar

Supplementary Figures

1. Spatial distribution of study sites in this study
2. Interpolation and extrapolation capacity assessment for the major and second rice growing season based on subsets of soil water potential and field water depth
3. Relationships between ΔY and predictors

31. Predicted ΔY in response to soil water potential thresholds under different levels of mean growing season temperature and climatological water availability

Supplementary Text 1 Potential physiological mechanisms of AWD-induced ΔY

To understand potential physiological mechanisms of ΔY, we first summarized essential physiological processes that are responsible for ΔY through literature review (Table S6). Accordingly, observations on nine related physiological traits were collected in the data compilation process, including total biomass production (TB), ratio of aboveground biomass to total biomass (ABF), harvest index (HI), total nitrogen uptake (NUP), leaf area index (LAI), maximum tillers (MTI), root biomass (RTW), photosynthetic rate (PNR), and contribution of post-heading Nonstructural Carbohydrate to grains (NSC) (Table S2). In total, we collected 542 paired observations for TB, 542 for ABF, 542 for HI, 269 for NUP, 182 for LAI, 123 for MTI, 204 for RTW, 59 for PNR, and 68 for NSC.

First, we investigated the relationships between changes in yield, yield components and environmental and management-related drivers. We found that yield tended to increase under conditions with relatively high climatological water availability (CWA, cumulative precipitation minus crop evapotranspiration during growing season) and on acidic and less sandy soils, and when the lowest threshold of soil water potential was relatively high (Fig. S6). Both total biomass production and harvest index tend to increase under such circumstances. Moreover, the changes in total biomass production were more sensitive to these drivers compared to changes in harvest index. This explains the cases of yield increase or maintenance when increase in harvest index offset the loss in total biomass production.

Second, to further investigate the potential physiological processes underlying yield changes, we analyzed the correlations between changes in physiological traits and yield components. We identified three pathways that could help explain the yield increment under beneficial conditions from physiological perspectives. (1) Synergy pathway: LAI tended to increase to a larger extent under the beneficial conditions (i.e., higher CWA, lower soil pH and sand contents, higher soil water potential threshold, Fig. S7), therefore contributed to increase in both total biomass production and harvest index (Fig. S10). (2) Compensate pathway: Larger NSC tended to occur at acidic and less sandy soils, contributing to larger increase in harvest index. This pathway helps to explain yield increase cases when increase in harvest index compensated decrease in total biomass production. (3) Tradeoff pathway: The changes in total biomass production and harvest index correlated conversely with changes in NUP and MTI. Therefore, under conditions of acidic soils and lower soil water potential threshold, larger reduction in NUP and MTI would correspond to larger increase in harvest index while larger reduction in total biomass production. By contrast, under conditions of higher CWA, larger increase in NUP would correspond to larger increase in total biomass production while larger reduction in harvest index. These results highlight the importance of coordination between total biomass production and harvest index for yield increase.

Finally, we used a series of Structural Equation Models (SEMs) to investigate the direct or indirect correlations among predictors, changes in physiological traits and yield. Modelling results suggested ΔNUP as a potentially important trait regulating ΔTB under combined effects of soil water potential, AWD upper threshold and climatological water availability (Fig. S11). This is probably associated with soil water and N interactions (e.g., ammonia volatilization, nitrification and denitrification) and root-soil interactions that influence nitrogen availability and thus nitrogen uptake [1, 2]. It should be noted that the SEMs were developed based on different subsets depending on available observation number of physiological traits, so their performance can not be compared. As a consequence, the predominant physiological process underlying ΔY can not be determined. This requires further experiments with simultaneous measurement of multiple physiological traits.

Supplementary Text 2 Relations between field water depth and soil water potential

To convert field water depth to soil water potential, we reproduced their relationships based on 836 simultaneous field observations of field water depth and soil water potential using two kinds of approaches: empirical nonlinear statistical models and a process-based model (soil water heat carbon nitrogen simulator (WHCNS))[3]. Only seven studies spanning 11 sites were selected, forming 20 site×year×AWD treatment groups (Table S7). This is because most studies only used one of the indicators to monitor soil water statue. Daily observations of soil water potential and field water depth were extracted by GetData.

(1) Empirical nonlinear statistical models

We used two forms of empirical statistical models to quantify relationships between field water depth and soil water potential, that is, power and exponential function (Equation 1 and 2). The power function was derived from the widely used power function between soil water content and soil water potential (soil water retention curve), and linear function between soil water content and field water depth used by a previous study [4]. The exponential form was used following a previous study [5]. We conducted similar procedure of model calibration and prediction based on both functions as below.

First, we fitted the basic function based on observations from each group of site×year×AWD treatment individually to calibrate parameter *a* and *b* (Equation 1 and 2) (Table S8). Both parameter *a* and *b* varied across groups depending on varying hydrological and soil conditions across sites and years [6]. Therefore, we connected the calibrated parameters *a* and *b* with site-specific climate conditions and soil properties (N=20), and found significant relationship between *a* and growing season precipitation (log-transformed), and *b* with soil sand fraction, regardless of power or exponential function (Fig. S27-28). We incorporated the role of season precipitation and soil sand content to modify model forms (Equation 3 and 4) and re-calibrated the parameters a_1, a_2, b_1 and b_2 based on all observations (N=836). Fourth, combing the well-calibrated model (Table S9 and Fig.S25) and spatial explicitly information of growing season temperature and soil sand fraction, we predicted gridded soil water potential corresponding to field water depth at 15cm below soil surface (Fig. S14).

$$SWP = a \cdot \left|FWD\right|^{b} \tag{1}$$

$$SWP = c \times (1 - \exp(d \times FWD)) \tag{2}$$

$$SWP = (a_1 \times \log(P) + a_2) \cdot \left|FWD\right|^{(b_1 \times sand + b_2)} \tag{3}$$

$$SWP = (c_1 \times \log(P) + c_2) \times (1 - \exp((d_1 \times sand + d_2) \times FWD)) \tag{4}$$

where SWP represents soil water potential (kpa), FWD represents field water depth (cm), P is total precipitation during rice growing season (mm), and $sand$ represents soil sand content (%). a_1, a_2, b_1, b_2, c_1, c_2, d_1, d_2 are empirical parameters calibrated using a least-squares error technique.

(2) Process-based model (*WHCNS*)

Soil water component in WHCNS model. We used an integrated soil-crop system model, WHCNS, to simulate daily soil water dynamics and reproduce the relationship between field water depth and soil water content at the daily scale. In this model, reference evapotranspiration was computed using the Penman–Monteith method[7]. The crop coefficient was used to calculate actual crop potential evaporation. And then potential crop transpiration and potential soil evaporation was separated using leaf area index (LAI). Soil water infiltration after rainfall or irrigation events was simulated by a modified Green–Ampt equation[8]. The redistribution of soil water under different upper and low boundaries was simulated using Richards' equation. Relationship between soil water content and soil water potential was described by the van Genuchten-Mualem model (1980)[9]. This model facilitates the calculation and output of both soil water content and soil water potential for soils with stratified layers.

Model setup and modelling. To drive the WHCHS model, input data includes daily meteorological variables (i.e., mean, maximum and minimum air temperature, wind speed, precipitation, humidity, downward solar radiation), soil properties by depth (i.e., bulk density, field capacity, soil water content, wilting point, soil texture, saturated hydraulic conductivity) and daily lowest and upper irrigation threshold. We acquired daily meteorological variables and soil properties from the ERA5[10] and SoilGrids dataset [11], respectively. We setup daily lowest and upper irrigation threshold based on the descriptions reported by the original study. For global predictions, daily lowest and upper irrigation were set as −50 kpa and 5 cm for each grid at 0.5-degree spatial resolution. Based on model simulated daily soil water content and soil water potential by depth, we calculated daily field water depth using Equation 5.

$$FWD = \frac{\sum_{i=1}^{I}(\theta_i - \theta_{f,i}) \times D_i}{\sum_{i=1}^{I}(\theta_{s,i} - \theta_{f,i}) \times D_i} \times \sum_{i=1}^{I} D_i - \sum_{i=1}^{I} D_i \tag{5}$$

where FWD represents field water depth (cm). $\theta_{15\text{-}20}$ and θ_i represents soil water content at soil depth of 15-20-cm and at soil layer i ($cm^3\ cm^{-3}$) that were simulated by WHCNS. $\theta_{s,i}$ and $\theta_{f,i}$ represent saturated soil water content and field capacity at soil layer i ($cm^3\ cm^{-3}$). I represents the soil layer corresponding to 15-20-cm soil depth. D represents monitoring depth of the field water, obtained from the original article and set as 15 cm for global prediction. α, m and l are shape parameters of the van Genuchten model, calibrated based on the paired observations of SWP and FWD.

(3) Comparisons

We compared the differences among the three approaches from aspects of (1) model performance, (2) predicted soil water potential at field water depth of −15cm, and (3) identified priority areas and predicted water productivity improvements for applying the soil water potential-based AWD scheme. First, all of the three approaches performed satisfactorily for converting field water depth into soil water potential (Table S9, Fig. S14, R^2 = 0.76 and *nRMSE* = 6.3% using power function, R^2= 0.81, *nRMSE* = 5.6% using exponential function, R^2 = 0.72 and *nRMSE* = 11.8% using power function). Second, the predicted soil water potential corresponds to −15 cm field water depth showed descending order using power function, exponential function and process-based model (e.g., −5.4, −6.5 and −8.7 kpa). Nonetheless, these estimates all coincided with previous studies in that soil water potential is higher than −10 kpa at field water depth higher than −15 cm (Table S14 and Fig. S14) [2, 5, 12]. Finally, despite differences in the predicted soil water potential, priority areas for the soil water potential-based AWD were consistent using either approaches, covering 37% of the global irrigated harvested areas. These results suggested that approach chosen would not bias our main findings, that is, setting spatially explicit soil water potential threshold for AWD application is a promising pathway to increase water productivity while maintaining yield. In the main text, we used the median estimates using the three approaches.

Supplementary Text 3 Calculation of water stress index

Water stress index (WSI) was calculated at spatial resolution of 0.5° (re-gridded to 5′) following the definition of SDG Indicator 6.4.2 (Level of water stress: freshwater withdrawal as a proportion of available freshwater resources) by United Nations [13].

$$\mathrm{WSI}_{i,y}(\%)=\frac{TFWW_{i,y}}{TRWR_{i,y}-EFR_{i,y}}\times 100\%$$

$$TFWW_{i,y}=IRR_{i,y}+IND_{i,y}+DOM_{i,y}$$

$$TRWR=Q_{loc,i,y}+discharge_{i,y}$$

$$\begin{cases} EFR_{i,m}=0.6\times MMF_{i,m}, & if \quad MMF_{i,m}\le 0.4\times MAF_i \\ EFR_{i,m}=0.3\times MMF_{i,m}, & if \quad MMF_{i,m}>0.8\times MAF_i \\ EFR_{i,m}=0.45\times MMF_{i,m}, & if \quad 0.4\times MAF_i\le MMF_{i,m}\le 0.8\times MAF_i \end{cases}$$

Where $TFWW_{i,y}$ is total volume of fresh water extracted from its sources for cell i in year y, encompassing irrigation (IRR), industrial (IND) and domestic (DOM) sectors in this study. $TRWR_{i,y}$ is total renewable water resources, calculated by the sum of local runoff ($Q_{loc,i}$) and incoming discharge from the upstream cells ($discharge_{i,y}$). ERF is environmental requirement flow, with monthly values first calculated based on the variable monthly flow method (VMF) using monthly natural ($MMF_{i,m}$) flow [14]. Then monthly EFR was aggerated to obtain annual values. All data (including IRR, IND, DOM, Q_{loc}, $discharge$ and MMF) were obtained from an ensemble of four Global Hydrological Models (i.e., H08, LPJmL MATSIRO and PCR-GLOBWB) participating the Inter-Sectoral Impact Model Intercomparison Project (ISIMIP 2a) forced by three meteorological datasets (i.e., GSWP3, WFDEI, Princeton) (see Table S5 for dataset used). All variables are expresses in km^3 year^{-1}.

According to United Nation, water stress is classified into no (WSI<25%), low (25%<WSI<50%), medium (50%<WSI<75%), high (75%<WSI<100%) and critical (WSI>100%) levels according to WSI values [13].

Supplementary Tables

Table S1 Comparison of AWD effects on rice yield (ΔY) between this study and previous studies

Reference	AWD scheme	Sample number	Study number	ΔY
This study	Soil water potential (744) Field water depth (523) Both (85)	1187	123	−2.9% (5^{th} – 95^{th} percentile: −30.5 to 22.1%)
Zhang et al., 2023[15]	Soil water potential Field water depth	1025	117	−6% (95% CI: −9 to −3%)
Cheng et al., 2023[16]	Field water depth	176	22	−2.5 ± 15%
Ishfaq et al., 2020[17]	Soil water potential Field water depth	45	21	−5.1 ±15.1%
Jiang et al., 2019[18]	Soil water potential Field water depth	160	41	−3.6 %
Carrijo et al., 2017[2]	Soil water potential Field water depth	524	56	−5.4% (95% CI: −8.7 to −1.8%)

Table S2 List of variables included in this study

Type	Variable	Unit
Target variables	Rice yield [Y] (n = 1,187, including 744 for Soil water potential and 523 for field water depth)	kg ha^{-1}
	Irrigation water use [IRR] (n = 233)	mm
	Yield component: Total Biomass production [TB] (n = 332) Aboveground biomass fraction [ABF] (n = 332) HI-Harvest Index [HI] (n = 332) **Production:** Root Weight [RTW] (n = 99) Leaf Area Index [LAI] (n = 155) MTi- Maximum number of tillers [MTI] (n = 99) **Nitrogen metabolism:** Total crop nitrogen uptake [NUP] (n = 136) **Allocation:** Nonstructural Carbohydrate remobilization [NSC] (n = 68) **Functional:** Photosynthetic rate [PNR] (n = 59)	 kg ha^{-1} – – kg ha^{-1} m^2 m^{-2} kg ha^{-1} kg N ha^{-1} % μmol CO_2 m^{-2} s^{-1}
Agricultural Management practices	Soil water potential at 15-20-cm soil depth [SWP]	kpa
	Field water depth below soil surface [FWD]	cm
	Upper threshold of AWD [U_{AWD}]	cm
	Nitrogen application rate [Nrate]	kg N ha^{-1}
Climate	Growing season temperature [T]	°C
	Climatological water availability: growing season precipitation minus growing season crop potential evapotranspiration [CWA]	mm
Soil	Soil pH [pH]	–
	Soil sand content [Sand]	%
Experimental parameters	Geographical location (Latitude, Longitude)	Degree
	Altitude of experimental sites [Altitude]	m
	Experimental replicated times	–
	Experimental duration	day
	Experimental start and end date	–
Interaction terms	SWP: T, SWP: CWA, SWP: pH, SWP: Sand, SWP: U_{AWD}, SWP: Altitude, U_{AWD}: T, U_{AWD}: CWA, U_{AWD}: Sand	–

Table S3 Model details for predicting AWD effects on yield (ΔY model, ln-transformed effect size was used as dependent variables for modelling, $R^2 = 0.43$, $n = 719$, $p < 0.001$, RMSE = 12%). The significance of parameters was based on the t statistics using a two-tailed test.

Parameter	Estimate	Std.error	t value	Pr
Intercept	-0.02	0.03	-0.60	0.55
scale(SWP)	0.66	0.03	19.29	< 0.001
scale(T)	0.10	0.03	3.48	< 0.001
scale (pH)	-0.10	0.03	-3.37	< 0.001
scale(U_{AWD})	-0.18	0.03	-6.16	< 0.001
scale(SWP)×scale(CWA)	0.17	0.03	5.89	< 0.001
scale(SWP)×scale(Sand)	0.12	0.02	5.99	< 0.001
scale(SWP)×scale(Altitude)	-0.07	0.03	-2.38	< 0.001

Table S4 Model details for predicting AWD effects on irrigation water use (ΔIRR model, ln-transformed effect size was used as dependent variables for modelling, $R^2 = 0.41$, $n = 233$, $p < 0.001$, RMSE = 14%). The significance of parameters was based on the t statistics using a two-tailed test.

Parameter	**Estimate**	**Std.error**	**t value**	**Pr**
Intercept	0.00	0.06	0.01	1.00
scale(SWP)	0.57	0.06	9.70	<0.001
scale(U_{AWD})	0.19	0.06	3.12	0.002
scale(CWA)	-0.11	0.06	-1.90	0.059
scale(SWP)×scale(U_{AWD})	-0.11	0.06	-1.74	0.083
scale(SWP)×scale(CWA)	0.24	0.05	4.55	<0.001
scale(SWP)×scale(T)	0.11	0.06	1.85	0.065
scale(U_{AWD})×scale(CWA)	0.16	0.06	2.51	0.013
scale(U_{AWD})×scale(T)	0.15	0.05	2.84	0.005
scale(U_{AWD})×scale(Sand)	-0.14	0.06	-2.40	0.017

Table S5 Global Hydrological models used for calculating water stress index (WSI)

Model name	Climate forcing	Output variables used	Reference
H08	GSWP3, WFDEI, Princeton	dis, qtot, airrww, adomww, amanww	[19, 20]
LpjmL		dis, qtot, airrww	[21, 22]
MATSIRO		dis, qtot, airrww, adomww, amanww	[23]
PCR-GLOBWB		dis, qtot, airrww, adomww, amanww	[24, 25]

Table S6 Summary of physiological processes underlying AWD effects on rice yield proposed by previous studies

Mechanisms	Physiological traits	Processes
Enhancement in root growth→total biomass production [TB] & aboveground biomass faction [ABF]	Root dry weight [RTW] Root oxidation activity [ROA] Total N uptake [NUP]	1. AWD would influence root growth and activity to influence supply of nutrients and water for photosynthesis, biomass production, allocation ratio between root and shoot, and shoot growth [26, 27] 2. AWD would impact synthesis of plant hormones of roots to regulate the other physiological responses [28]
Improved shoot growth and canopy structure → TB &Harvested index [HI]	Maximum number of tillers [MTI] Leaf Area Index [LAI] Leaf photosynthetic rate [PNR] Angle of top three leaves Total N uptake [NUP]	1. Reducing redundant vegetative growth by reducing MTI, while increasing percentage of productive tillers to optimize canopy architecture [29] 2. Appropriate LAI to coordinate source-sink relationship [27] 3. Reducing leaf ANGLE of top three leaves to coordinate the distribution of light and N within the canopy to maximize canopy photosynthesis [27, 30] 4. AWD would induce alterations in N metabolism, including NUP (primarily in leaf), leaf N allocation between photosynthetic and non-photosynthetic apparatus, and among the components of the photosynthetic apparatus, to coordinate drought tolerance and photosynthesis acclimation of leaves [31]
Enhanced remobilization of carbon reserves from stems to grain→ HI	NSC remobilization rate [NSC], ratio of nonstructural carbohydrate in vegetative tissues remobilized and transferred to grains in the grain-filling period	1. AWD would enhance activities of α-amylase and sucrose-phosphate synthase leading to the fast hydrolysis of starch and increased carbon remobilization in the source side (stem) 2. AWD would increase/decrease activities of key enzymes involved in sucrose-to-starch conversion in the grains to influence grain-filling rate and starch accumulation rate in the sink side (grains) [27, 29, 32]

Table S7 Information of experiments used for parameter calibration of the empirical models between field water depth and soil water potential

ID	Site	Country	Longitude	Latitude	Treatment	Start Date	Harvest Date
1	1	The Philippines	120.9	15.7	AWD15	2010/1/12	2010/4/19
2	1	The Philippines	120.9	15.7	AWD25	2010/1/12	2010/4/19
3	1	The Philippines	120.9	15.7	AWD35	2010/1/12	2010/4/19
4	1	The Philippines	120.9	15.7	AWD35	2011/1/4	2011/4/16
5	1	The Philippines	120.9	15.7	AWD25	2011/1/4	2011/4/16
6	1	The Philippines	120.9	15.7	AWD15	2011/1/4	2011/4/16
7	2	China	113.3	23.1	AWD30	2014/8/12	2014/11/10
8	2	China	113.3	23.1	AWD15	2014/8/12	2014/11/10
9	2	China	113.3	23.1	FP	2014/8/12	2014/11/10
10	3	USA	-121.7	39.5	AWD35	2016/5/24	2016/10/20
11	4	Kenya	37.4	-0.7	AWD20cm	2015/9/9	2016/1/17
12	4	Kenya	37.4	-0.7	AWD20cm	2016/10/1	2017/1/30
13	4	Kenya	37.4	-0.7	AWD20cm	2017/7/23	2017/11/20
14	5	The Philippines	120.9	15.7	ASNS	2001/1/13	2001/4/23
15	6	China	114.5	30.5	AWD&D	2016/6/25	2016/9/14
16	7	Colombia	-75.2	4.4	AWD30	2017/12/1	2018/2/1
17	8	Colombia	-75.1	4.3	AWD30	2018/2/15	2018/4/18
18	9	Colombia	-75.2	4.4	AWD30	2018/1/29	2018/4/1
19	10	Colombia	-75.1	4.4	AWD30	2017/10/15	2017/12/16
20	11	The Philippines	121.4	14.3	AWD	2002/1/6	2002/4/26

Table S8 Calibrated parameters from each group of site×year×AWD treatment observations

ID	N	$SWP=a\times\|FWD\|^b$			$SWP=a*(1-\exp(b\times FWD))$		
		a	**b**	R^2	**a**	**b**	R^2
1	27	0.66	1.04	0.76	2.42	-0.12	0.52
2	40	0.51	1.12	0.93	12.66	-0.04	0.84
3	31	0.70	1.04	0.90	24.15	-0.02	0.84
4	34	0.00	4.41	0.95	0.25	-0.18	0.94
5	28	0.12	1.58	0.83	4.02	-0.07	0.78
6	28	0.13	1.86	0.60	1.47	-0.20	0.49
7	112	0.00	2.67	0.72	1.49	-0.11	0.68
8	65	0.00	3.46	0.65	0.13	-0.26	0.64
9	95	0.00	3.35	0.79	0.21	-0.27	0.79
10	27	0.00	3.41	0.96	1.46	-0.10	0.95
11	15	0.01	1.82	0.92	0.33	-0.10	0.93
12	60	0.02	1.40	0.49	0.66	-0.07	0.50
13	41	0.00	2.78	0.74	0.03	-0.19	0.73
14	84	0.00	4.40	0.64	3.35	-0.05	0.80
15	23	0.15	1.53	0.77	13.63	-0.04	0.77
16	3	0.00	5.88	1.00	0.52	-0.19	1.00
17	3	0.00	6.12	1.00	0.69	-0.23	1.00
18	2	0.00	6.04	0.99	0.00	-0.23	1.00
19	3	0.00	5.22	1.00	1.01	-0.26	1.00
20	120	0.09	1.49	0.63	8.04	-0.03	0.64

Table S9 Calibrated model parameters and model performance of the empirical statistical models used to quantify relationships between field water depth and soil water potential based on power and exponential functions

Statistics	**Power function**	**Statistics**	**Exponential function**
a_1	-3.00E-04	c_1	-0.048
a_2	0.0074	c_2	2.23
b_1	0.0119	d_1	-1.40E-03
b_2	2.09	d_2	-0.04
R^2	0.76	R^2	0.81
nRMSE	6.3%	nRMSE	5.6%
N	836	N	836

Table S10 Probability distribution of model coefficients and input data for uncertainty estimation

Source	Probability distribution	Note
Input data (T, P, CWA)	Normal distribution	μ: value in ERA5 σ: 20% of μ assumed in this study
Input data (Altitude)	Normal distribution	μ: value in NOAA ETOPO dataset σ: 20% of μ assumed in this study
Input data (sand, pH)	Normal distribution	μ: value in Global Soil Dataset σ:difference between Global Soil Dataset and HWSD v1.2
Input data (Baseline of yield and irrigation for the major and second rice-growing season)	Normal distribution	μ: an ensemble mean of nine process-based crop models σ: 20% of μ assumed in this study
Model coefficients (ΔY model, ΔIRR model, FWD-SWP model)	Multivariate normal distribution	μ and σ were determined by corresponding fitted models

Table S11 List of studies in our database that explicitly recorded experimental conditions of weeds, insects and diseases. Either weeds, insects or diseases was reported in 6 studies colored pink below, while neither occurred in another 7 studies colored green below. In additional 64 out of 123 studies, strict management were imposed to avoid yield loss (e.g., diseases, insects, and weeds were strictly controlled during the entire growth period to avoid yield loss). No related information was mentioned in the rest 46 studies.

Reference	Country	Description
Singh et al., 2009 [33]	India	● Serious **root knot nematode infestation** was also a serious problem in transplanted rice on the **sandy loam** in the absence of continuous flooding. ● There was no evidence of rice root knot nematode infestation in any treatment on the **loam**.
Cabangon et al., 2011 [34]	Philippines	● The crop growth before PI was generally good in both years, but panicle damage, associated with the occurrence of deadhearts and whiteheads caused by Scirpophaga incertulas, was observed in both years.
Chidthaisong et al., 2018 [35]	Thailand	● blast disease (dry season of 2016)
Setyanto et al., 2018 [36]	Indonesia	● Pests, disease, and weeds were appropriately controlled ● Rice growth was generally normal, but in DS2, AWDS plots' rice plants were damaged by **rats**.
Setyanto et al., 2005 [37]	Indonesia	● In this study, there was no severe damage due to weed and rat, but the infestation by **stem borer** was severe, which lead to the low grain yield. ● the rice plants in all treatments were infested by stem borer during panicle initiation stage ● The infestation caused tiller destruction during panicle initiation stage, which reduced the number of effective tillers between 11% and 16%.
de Vries et al., 2010 [38]	Senegal	● No major pests or diseases were observed. ● No weed management in some of treatments.
Zhang et al., 2009 [26]	China	● No noticeable crop damage from weeds, insects, or diseases was observed in the experiments.
Zheng et al., 2018 [39]	China	● Insects and diseases were intensively

		controlled throughout the season with chemicals. Weeds were controlled manually. No noticeable crop damage was observed in either year.
Zheng et al., 2018 [40]	China	● Weeds, insects and diseases management were ● all in agreement with the local farmers' practices. No noticeable crop damage from weeds, insects and diseases was observed in the experiments in both years.
Li et al., 2022 [41]	China	● Weeds were removed manually when sighted. No obvious weed, pest or disease stress was observed during the rice-growing seasons.
Belder et al., 2004 [42]	China and Philippines	● Plots were regularly hand-weeded and pesticides were used to prevent insect and pest damage. No noticeable crop damage was observed in the experiments.
Devkota et al., 2013 [43]	Uzbekistan	● Weeds were not likely to have been a significant cause of the lower yield of the DSR treatments each year as they were effectively controlled through the combined use of post-emergence herbicide and hand weeding.
Howell et al., 2015 [44]	Nepal	● Although more weeds have been reported (but not quantified) in on- farm trials of AWD, in this experiment the opposite occurred. This could be related to the relatively shallow ponded water depths in CF plots (20–30 mm) and to soil contraction under AWD restricting weed growth as well as crop root development.

Table S12 Prediction of the lowest threshold of soil water potential, priority areas and water productivity improvements over the period of 2001-2015 based on two global soil datasets (Global Soil Dataset and Harmonized World Soil Database)

Year	Global Soil Dataset			Harmonized World Soil Database		
	Soil water potential threshold (kpa) median (5th –95th percentile)	**Priority areas (%)**	**ΔWater Productivity (%)**	**Soil water potential threshold (kpa) median (5th –95th percentile)**	**Priority areas (%)**	**ΔWater Productivity (%)**
2001	−18.5 (−23.7 to −4.6)	36.6	12.8	−17.2 (−20.5 to −4.1)	33.5	16.5
2002	−18.7 (−23.8 to −4.0)	37.0	12.5	−17.2 (−20.5 to −4.8)	34.1	15.6
2003	−18.7 (−23.8 to −4.1)	36.4	14.3	−17.4 (−20.5 to −4.3)	35.3	18.8
2004	−18.3 (−23.9 to −3.9)	36.9	11.5	−17.1 (−20.4 to −3.9)	34.3	15.0
2005	−18.7 (−23.0 to −3.8)	36.4	14.6	−17.4 (−20.6 to −4.6)	35.1	18.3
2006	−18.9 (−23.0 to −4.3)	37.0	13.3	−17.4 (−20.6 to −4.4)	34.7	16.4
2007	−18.7 (−23.5 to −4.6)	36.8	14.1	−17.4 (−20.5 to −4.0)	35.0	18.0
2008	−18.7 (−23.5 to −4.2	36.6	14.0	−17.4 (−20.5 to −4.5)	35.3	17.8
2009	−18.9 (−23.9 to −4.4)	36.6	14.0	−17.4 (−20.6 to −4.6)	35.9	17.2
2010	−19.1 (−23.9 to −4.8)	37.1	16.5	−17.7 (−20.7 to −5.1)	36.3	21.6
2011	−18.5 (−23.6 to −4.1)	36.0	14.3	−17.3 (−20.5 to −4.4)	35.8	18.0
2012	−18.7 (−23.9 to −4.4)	36.4	13.8	−17.4 (−20.6 to −4.8)	35.8	17.6
2013	−18.8 (−23.7 to −4.5)	35.9	15.1	−17.6 (−20.6 to −5.0)	35.7	18.5
2014	−18.7 (−24.0 to −4.2)	36.3	13.7	−17.3 (−23.7 to −4.8)	34.0	17.8
2015	−19.2 (−24.5 to −4.4)	36.9	14.1	−17.6 (−20.8 to −4.7)	34.2	18.8
Mean	**−18.7 (−23.8 to −4.3)**	**36.6**	**13.9**	**−17.4 (−20.6 to −4.5)**	**35.0**	**17.7**

Table S13 Changes in irrigation water use (ΔIRR) and water productivity (ΔWP) from adopting the soil water potential-based (SWP) and field water depth-based (FWD) AWD scheme, as compared to continuous flooding. The numbers in parentheses of the second column indicate the percentage of priority areas to the total irrigated rice harvested areas of the country. Relative changes were presented as mean [2.5% to 97.5% quantile as 95% prediction interval].

Country	**Priority area, %**	**ΔIRR, % (FWD) 1**	**ΔIRR, % (SWP) 2**	**ΔIRR, % (2-1)**	**ΔWP, % (FWD) 3**	**ΔWP, % (SWP) 4**	**Δ WP, % (4-3)**
India	15% (56%)	−33 [−39, −23]	−41 [−52, −35]	−8 [−23, −3]	56 [38, 68]	69 [54, 109]	13 [7, 52]
China	9% (32%)	−31 [−37, −22]	−45 [−52, −36]	−13[−23, −9]	59 [40, 76]	80 [56, 110]	21 [10, 53]
Bangladesh	4% (44%)	−32 [−39, −23]	−43 [−51, −34]	−12[−23, −3]	63 [44, 77]	77 [52, 104]	14 [2, 44]
Indonesia	2% (26%)	−30 [−37, −23]	−46 [−55, −34]	−16 [−27, −6]	61 [41, 75]	85 [51, 123]	24 [6, 62]
Thailand	1% (30%)	−29 [−39, −18]	−48 [−59, −33]	−19 [−32, −6]	65 [41, 85]	92 [48, 144]	28 [3, 78]
Pakistan	1% (44%)	−32 [−41, −18]	−39 [−60, −33]	−7 [−33, −2]	53[31, 78]	63 [49, 150]	10 [8, 92]
Vietnam	1% (18%)	−31 [−40, −21]	−50 [−62, −33]	−19 [−33, −8]	66 [40, 87]	98 [50, 160]	33 [3, 98]
Global	**37%**	**−32 [−38, −24]**	**−42 [−52, −36]**	**−10 [−24, −5]**	**60 [42, 70]**	**74 [55, 110]**	**13 [7, 52]**

Table S14 Results based on different approaches converting field water depth to soil water potential. See Supplementary Text 2 for details about the three approaches.

Method	**Field water depth threshold (kpa) median (5th –95th percentile)**	**Priority areas (%)**	**ΔIRR (%)**	**ΔWater Productivity (%)**
Power	−5.4 (−16.0 to −2.5)	37	−11	14
Exponential	−6.5 (−14.8 to −3.3)	37	−10	13
WHCNS	−8.7 (−11.8 to −1.7)	36	−8	11
Median	**−6.4 (−15.6 to −3.3)**	**37**	**−10**	**13**

Table S15 Sensitivity tests against rice cultivar. Three classifications of rice cultivar were considered to test its impacts: (1) Indica or Japonica rice, (2) upland or paddy rice, (3) inbred or hybrid rice. Considering record number of each class of cultivar, sensitivity tests were conducted based on five observational datasets: (1) all samples, (2) observations of Indica rice, (3) observations of Japonica rice, (4) observations of paddy rice (excluding that of upland rice), (5) observations of inbred rice (excluding that of hybrid rice). Also see Fig. S18 for comparisons.

Dataset	**N**	**Soil water potential threshold (kpa) median (5th –95th percentile)**	**Priority areas (%)**	**∆Water Productivity (%)**
All samples	719	−19.2 (−24.5 to −4.4)	37	14
Indica	456	−20.5 (−25.4 to −7.3)	34	18
Japonica	163	−15.7 (−17.6 to −9.7)	25	14
Paddy (excluding upland rice)	684	−19.2 (−24.6 to −4.4)	37	14
Inbred (excluding hybrid rice)	461	−18.8 (−25.5 to −4.6)	37	13

Supplementary Figures

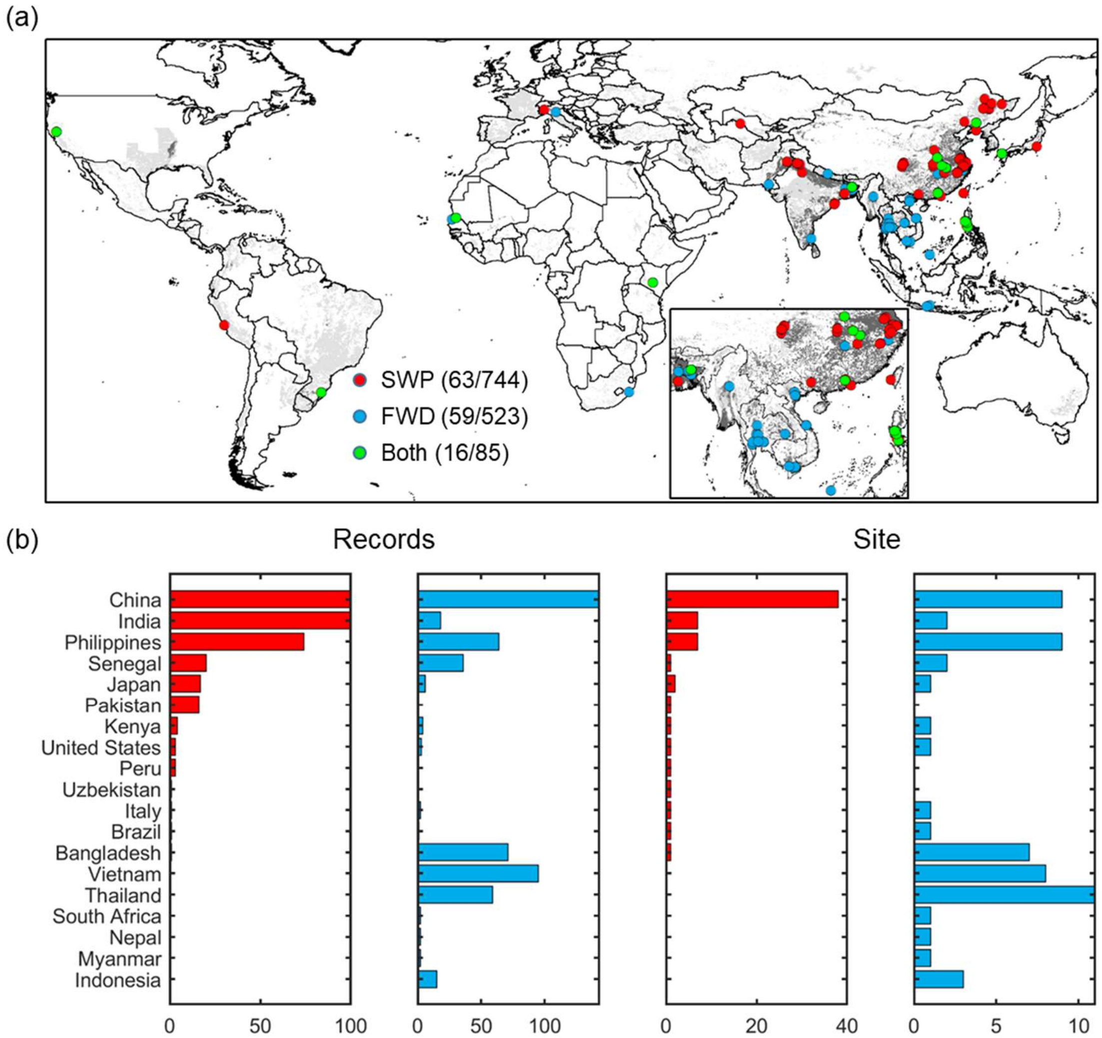

Fig. S1 Spatial distribution of study sites in this study. (a) The color of dots represents different metrics of soil moisture status: soil water potential (red), field water depth (blue) or both (green). The values in the parentheses are number of sites and paired observations. **(b)** Distribution of sites and data records in different countries. Experiments based on soil water potential were mostly in China, whereas experiments based on field water depth were widespread in Southeast Asia, possibly for the aim of testing the safe AWD scheme proposed by the IRRI. Base map of the country boundaries was obtained from Resource and Environmental Science Data Platform of China (https://www.resdc.cn/data.aspx?DATAID=205).

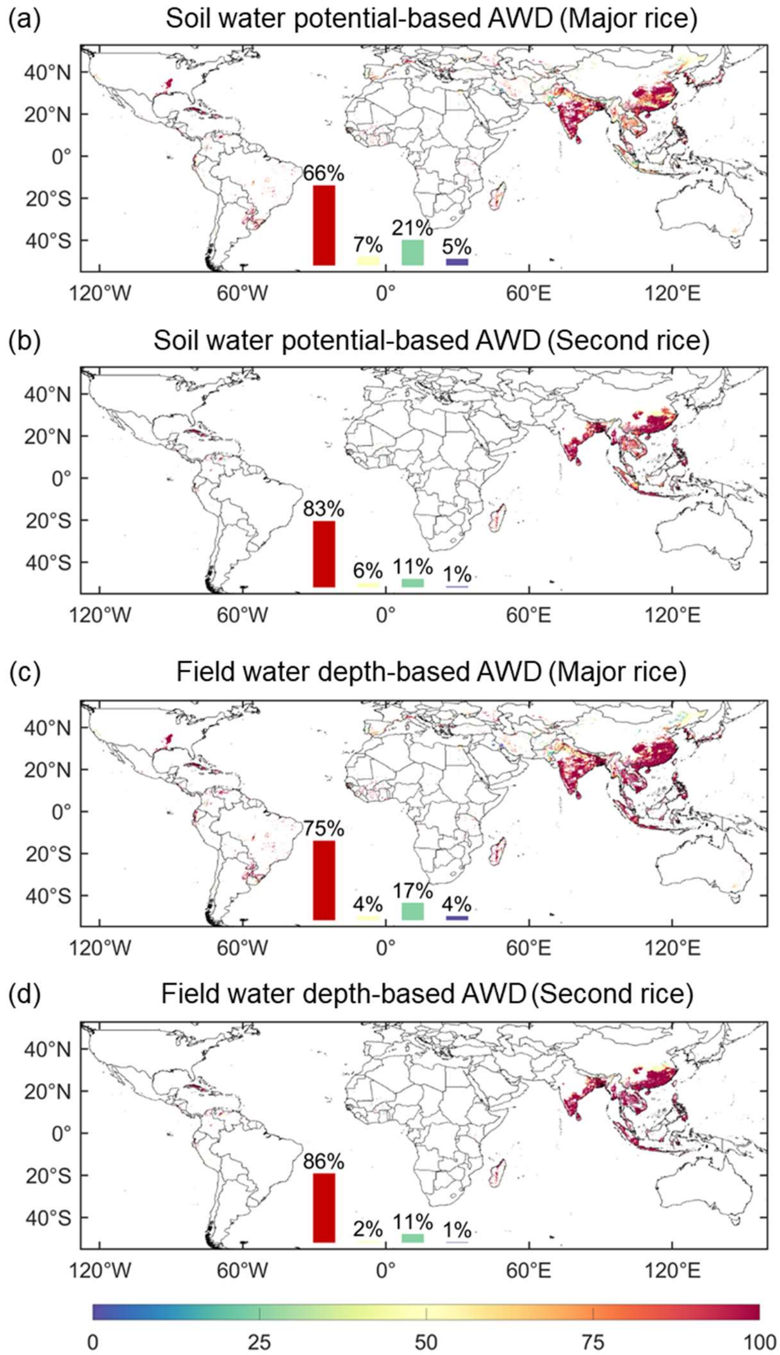

Fig. S2 Interpolation and extrapolation capacity assessment for the major (a, c) and second rice growing season (b, d) based on subsets of soil water potential (a-b) and field water depth (c-d). The calculation of interpolation percentage is based on the method of van den Hoogen et al. (2019). Low interpolation percentage (in blue) indicates that few global layers were represented by data, thus extrapolation would have occurred during prediction. High interpolation percentage (in red) is 'good' for our models as it indicates that many or all global layers were represented by data, thus interpolation would have occurred during prediction. Base map of the country boundaries was obtained from Resource and Environmental Science Data Platform of China (https://www.resdc.cn/data.aspx?DATAID=205).

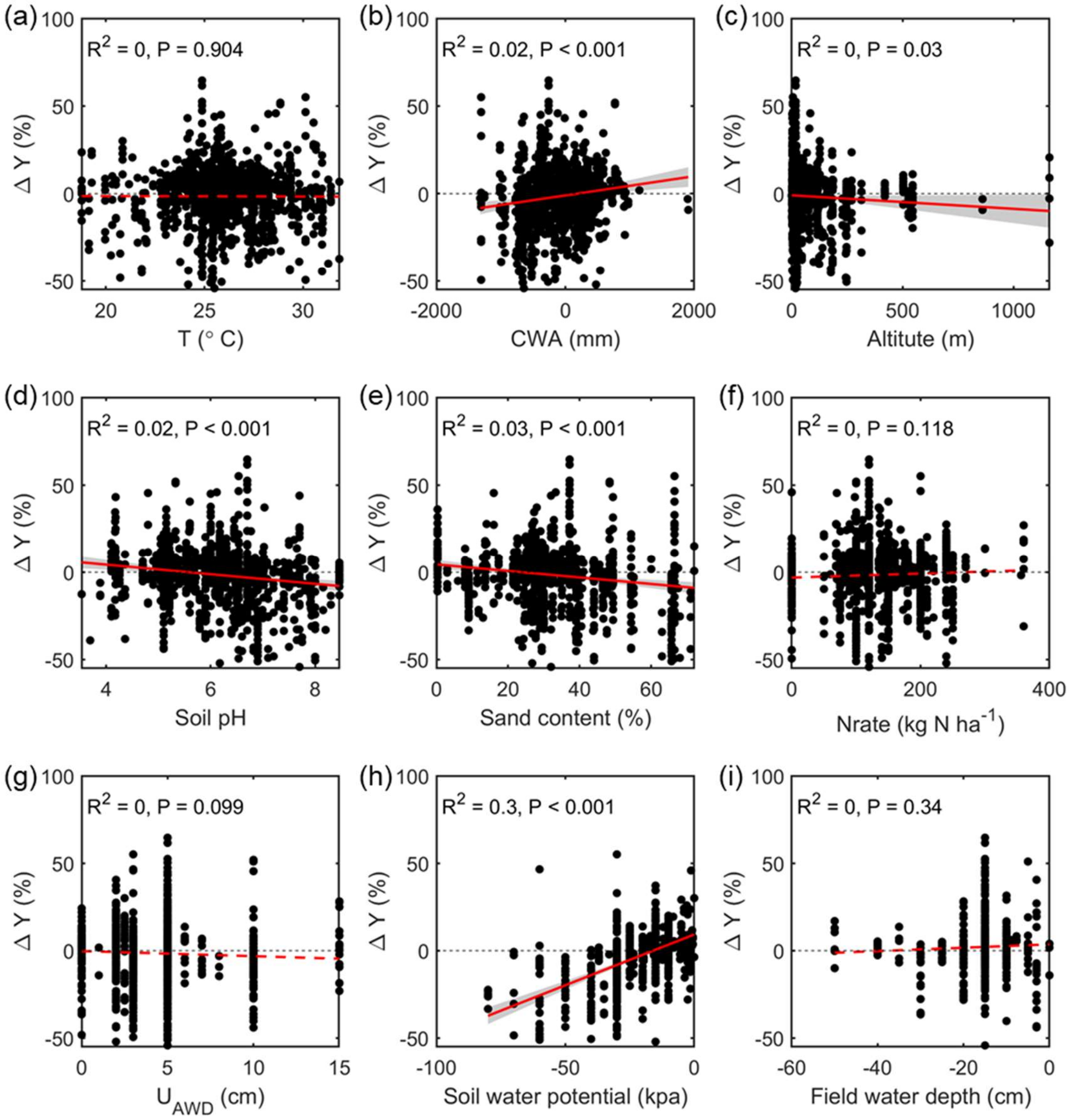

Fig. S3 Relationships between ΔY and predictors. (a) mean growing season temperature (*n* = 1187), **(b)** climatological water availability (*n* = 1187), **(c)** altitude (*n* = 1187), **(d)** soil pH (*n* = 1187)**, (e)** soil sand content (*n* = 1187)**, (f)** nitrogen application rate (*n* = 1187), **(g)** upper irrigation threshold (*n* = 1187), **(h)** soil water potential (*n* = 744), and **(i)** field water depth (*n* = 523). The red lines are regression lines with dashed lines indicating non-significant relationship ($P > 0.05$) based on two-sided t-test. Gray shading around each line represents the 95% confidence interval.

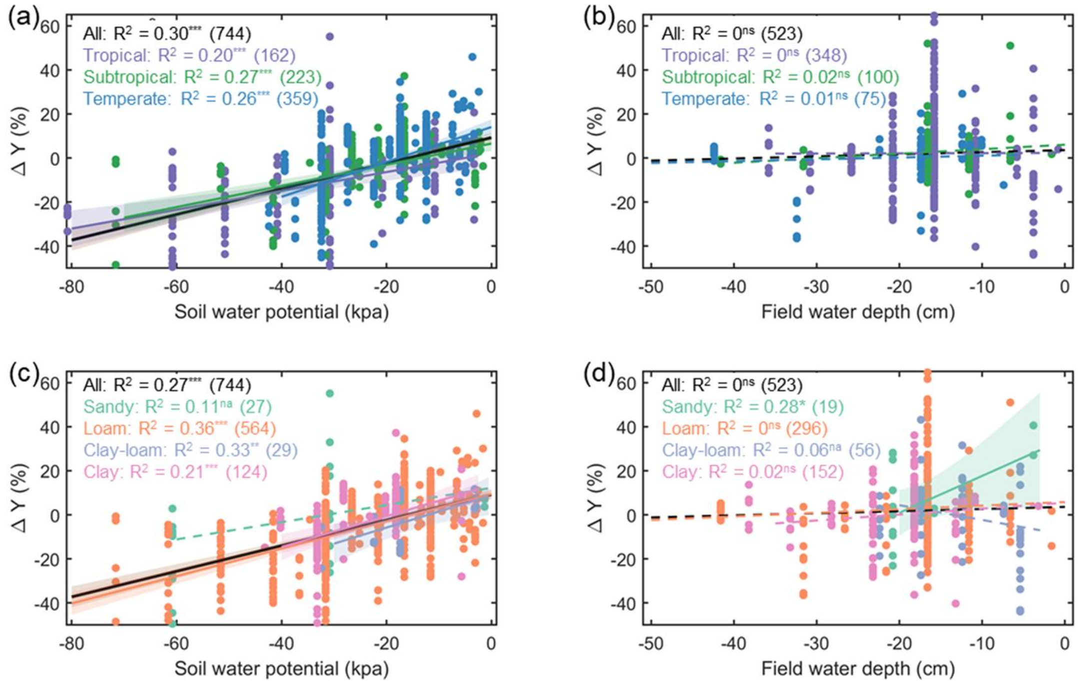

Fig. S4 Relationships between ΔY and the lowest soil water potential (a, c) or field water depth (b, d) for all observations and by different climatic zones (a-b) and soil textures (c-d). Asterisks indicate significance level of regression coefficient (i.e., *** $P < 0.001$, ** $P < 0.01$, * $P < 0.05$, ns $P > 0.05$). Numbers in parentheses indicate number of observations. The lines are regression lines with dashed lines indicating non-significant relationship ($P > 0.05$) based on two-sided t-test. Shading areas around each line represents the 95% confidence interval.

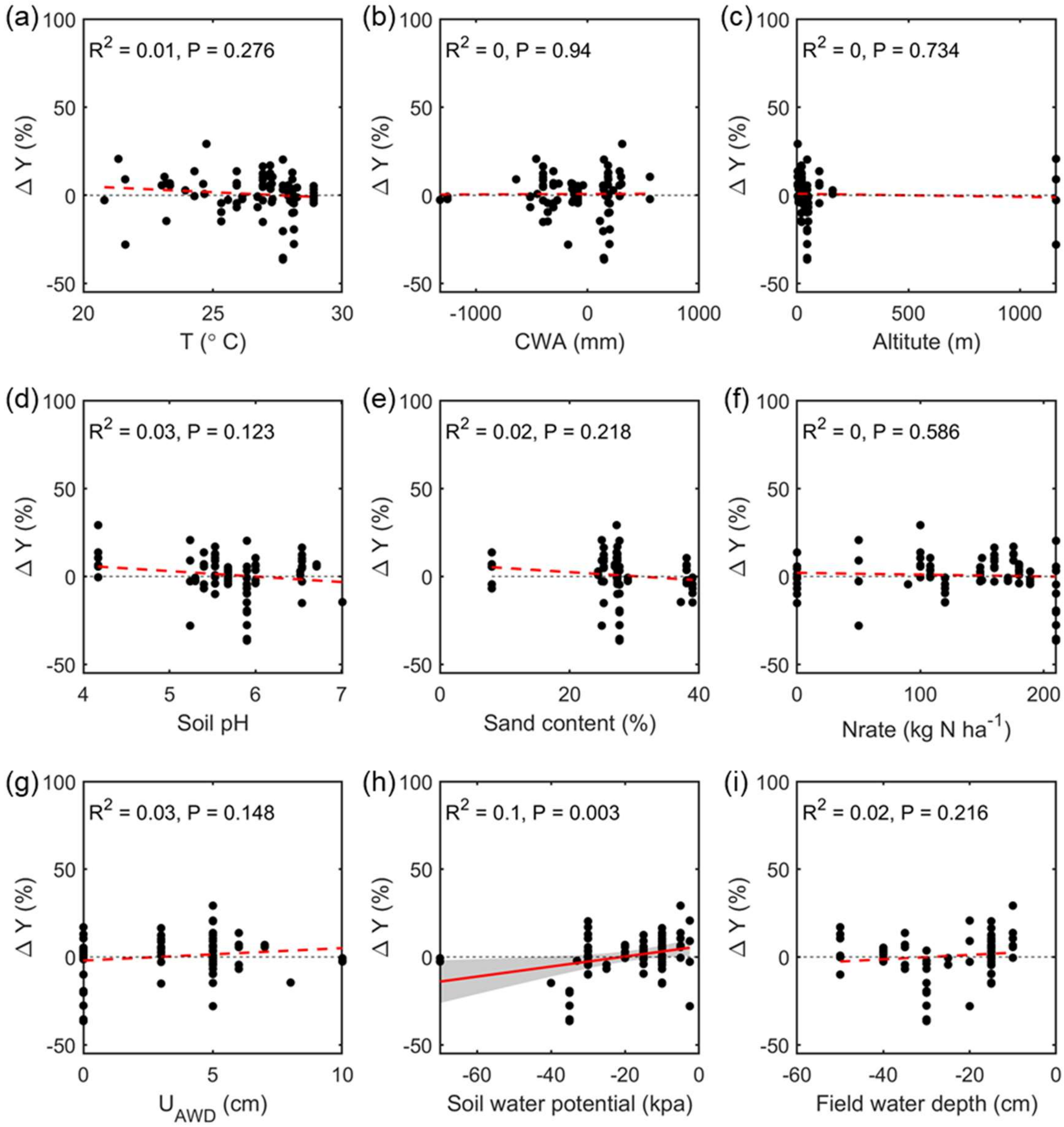

Fig. S5 Relationships between ΔY and predictors based on observations with simultaneous measurements of soil water potential and field water depth (*n* = 85 from 12 studies). (a) mean growing season temperature, **(b)** climatological water availability, **(c)** altitude, **(d)** soil pH**, (e)** soil sand content**, (f)** nitrogen application rate, **(g)** upper irrigation threshold, **(h)** soil water potential, and **(i)** field water depth. The red lines are regression lines with dashed lines indicating non-significant relationship ($P > 0.05$) based on two-sided t-test. Gray shading around each line represents the 95% confidence interval.

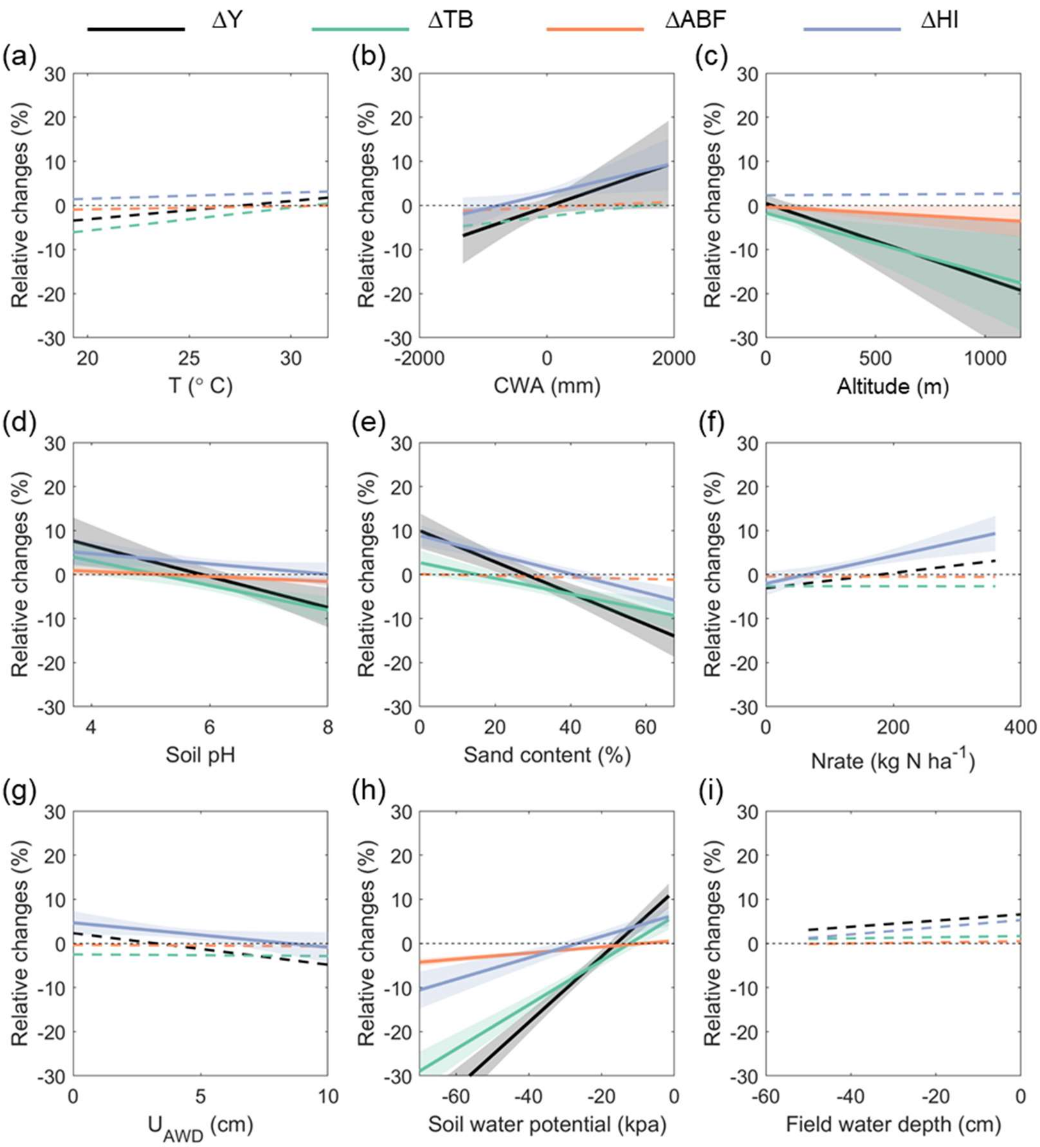

Fig. S6 Relationships between changes in yield and yield components and predictors. (a) mean growing season temperature, **(b)** climatological water availability, **(c)** altitude, **(d)** soil pH**, (e)** soil sand content, **(f)** nitrogen application rate, **(g)** upper irrigation threshold, **(h)** soil water potential, and **(i)** field water depth. The lines denote the regression lines, and the range of the error bands shows the 95% confidence intervals of the estimations of the regression model. Only fitted regression lines were shown with dashed lines indicating non-significant relationships ($P > 0.05$) based on two-sided t-test. ΔY, ΔTB, ΔABF and ΔHI represent relative changes in yield, total biomass production, ratio of aboveground biomass to total biomass, and harvest index.

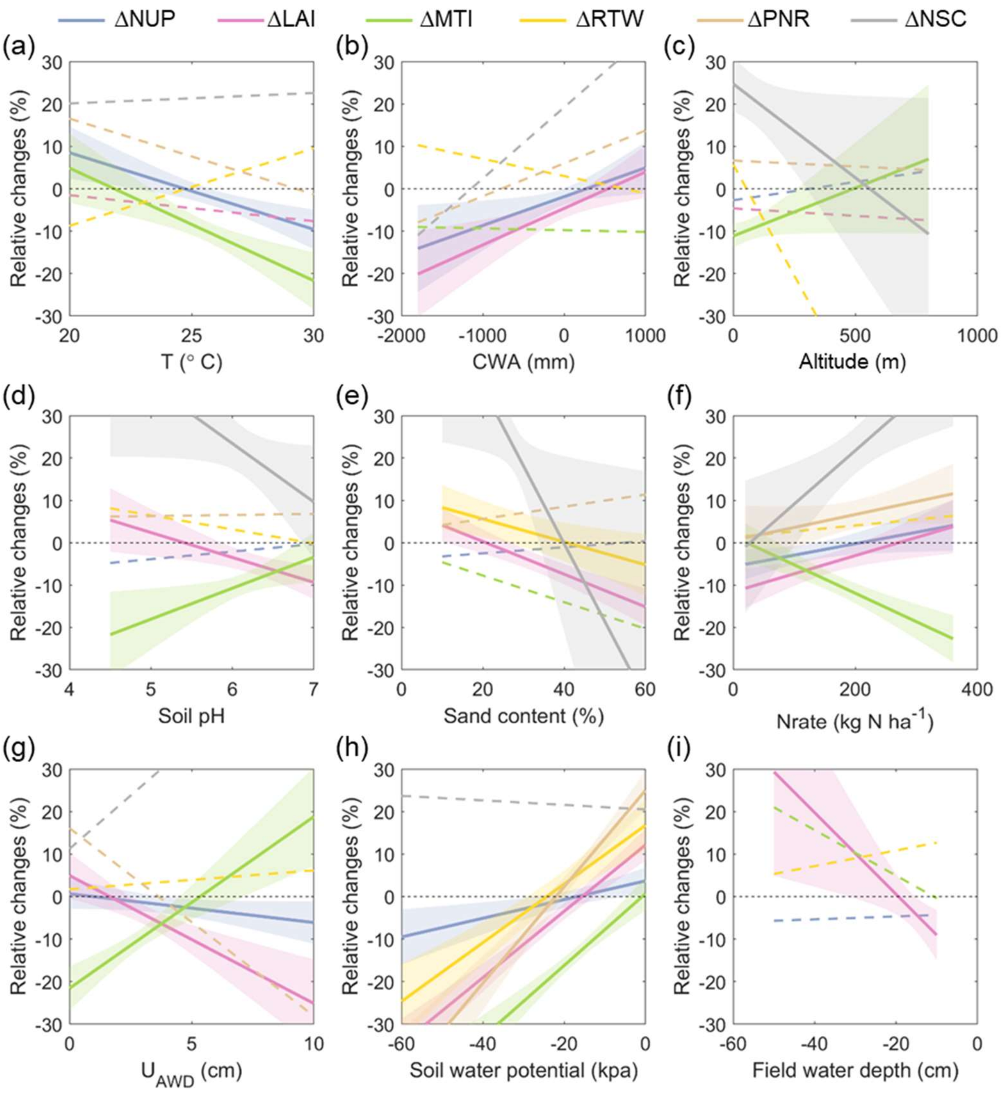

Fig. S7 Relationships between changes in physiological traits and predictors. (a) mean growing season temperature, **(b)** climatological water availability, **(c)** altitude, **(d)** soil pH**, (e)** soil sand content, **(f)** nitrogen application rate, **(g)** upper irrigation threshold, **(h)** soil water potential, and **(i)** field water depth. The lines denote the regression lines, and the range of the error bands shows the 95% confidence intervals of the estimations of the regression model. Only fitted regression lines were shown with dashed lines indicating non-significant relationship (P > 0.05) based on two-sided t-test. ΔNUP, ΔLAI, ΔMTI, ΔRTW, ΔPNR, and Δ NSC represent relative changes in total nitrogen uptake, leaf area index, maximum tillers, root biomass, photosynthetic rate, and contribution of post-heading Nonstructural Carbohydrate to grains.

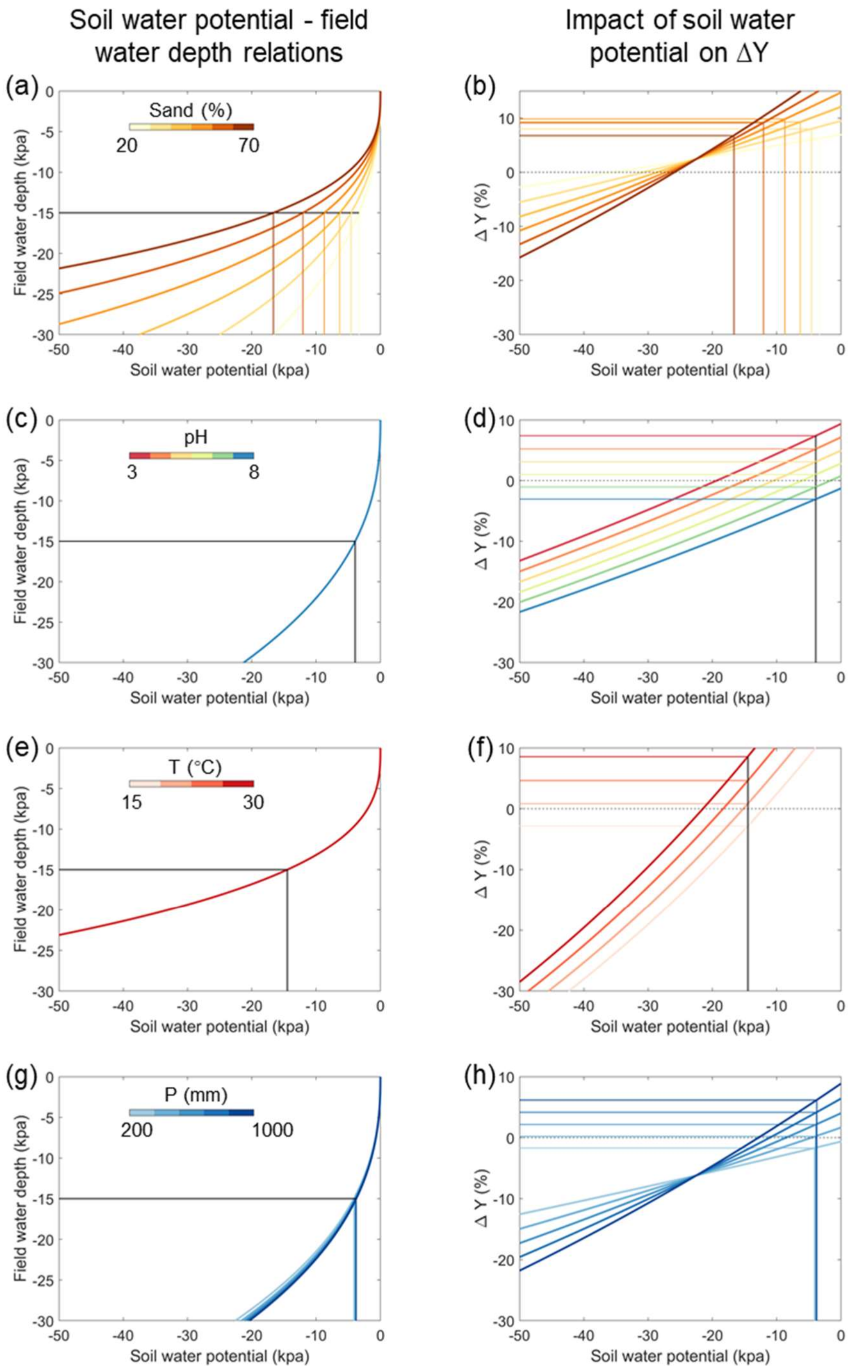

Fig. S8 Schematic illustration of differences in threshold and yield changes between soil water potential-based and field water depth-based AWD schemes. **(a, c, e, g)** show the simulated relationship between field water depth and soil water potential under different climate and soil conditions. These figures indicate that the −15cm field water depth threshold could correspond to a wide range of soil water potentials depending on environmental conditions. **(b, d, f, h)** show the simulated relationships between soil water potential and ΔY under conditions of the left panel. Vertical lines in all figures indicate soil water potential value correspond to −15cm field water depth. These figures were used to demonstrate how the fixed field water depth threshold (−15cm) could induce uncertain yield response under different environmental conditions.

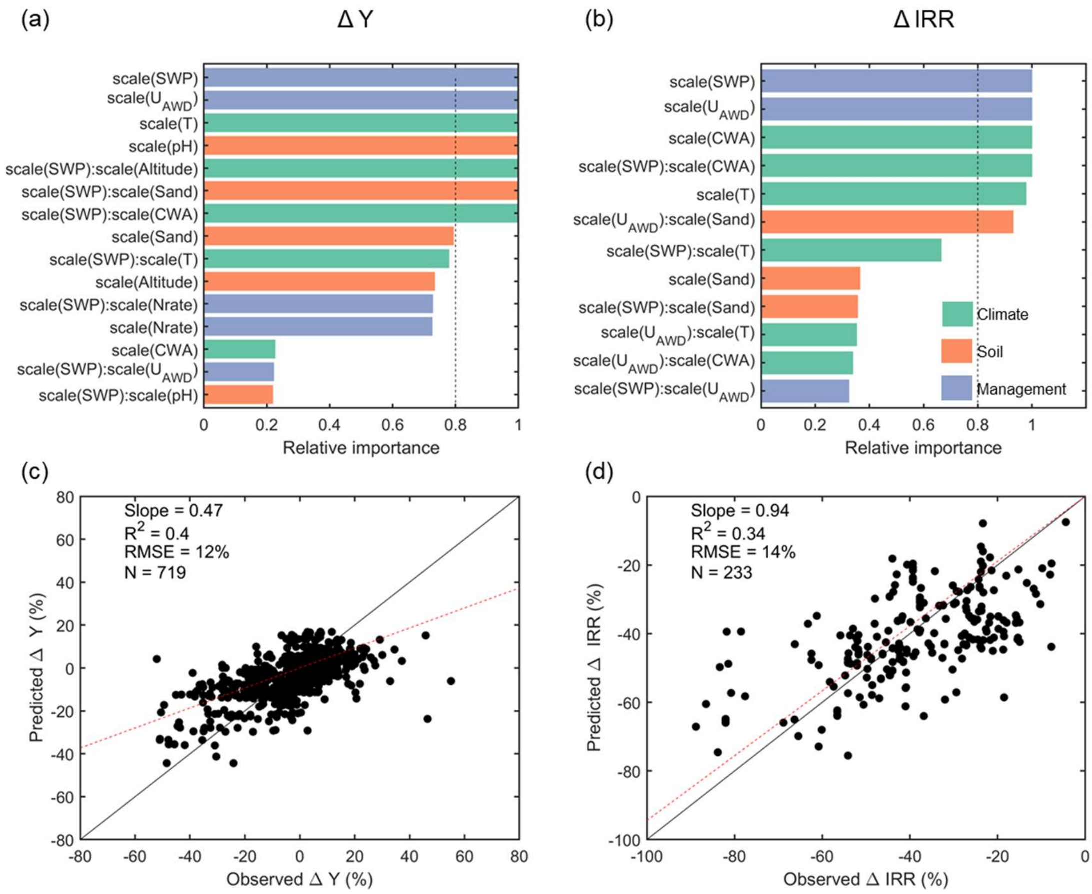

Fig. S9 Selection and performance of the ΔY and ΔIRR model. (a-b) Relative importance of potential predictors to variation in ΔY ($N = 719$) **(a)** and ΔIRR ($N = 233$) **(b)**. The importance is based on the sum of the Akaike weights derived from model selection using corrected Akaike information criterion. The cutoff is set at 0.8 to differentiate among the most important predictors (dashed lines). **(c-d)** Model performance from 50 times of five-fold cross validation. AWD effects on yield and irrigation water use were log-transformed as dependent variable (ln(ΔY/100+1) and ln(ΔIRR/100+1)) and transformed back into relative changes (%) after prediction.

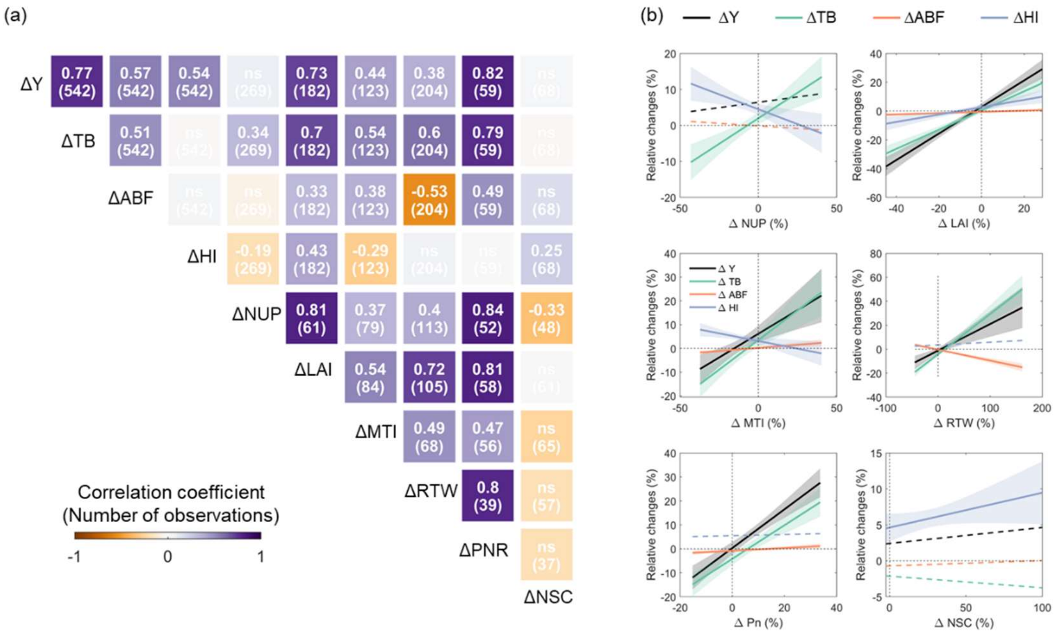

Fig. S10 Relationships between changes in yield, yield components and physiological traits. (a) Correlation coefficients between AWD effects on yield and physiological traits. Numbers represent Pearson's correlation coefficients ($P < 0.05$) and number of avaliable observations (in parentheses). Color indicates positive (purple) or negetive (brown) relationships. **(b)** Linear relationships between yield, yield components and physiological traits. The solid lines are regression lines, and the range of the error bands shows the 95% confidence intervals of the estimations of the regression model. Only fitted regression lines were shown with dashed lines indicating nonsignificant relationship ($P > 0.05$) based on two-sided t-test. ΔY, ΔTB, ΔABF, ΔHI, ΔNUP, ΔLAI, ΔMTI, ΔRTW, ΔPNR, and Δ NSC represent relative changes in total biomass production, ratio of aboveground biomass to total biomass, harvest index, total nitrogen uptake, leaf area index, maximum tillers, root biomass, photosynthetic rate, and contribution of post-heading Nonstructural Carbohydrate to grains.

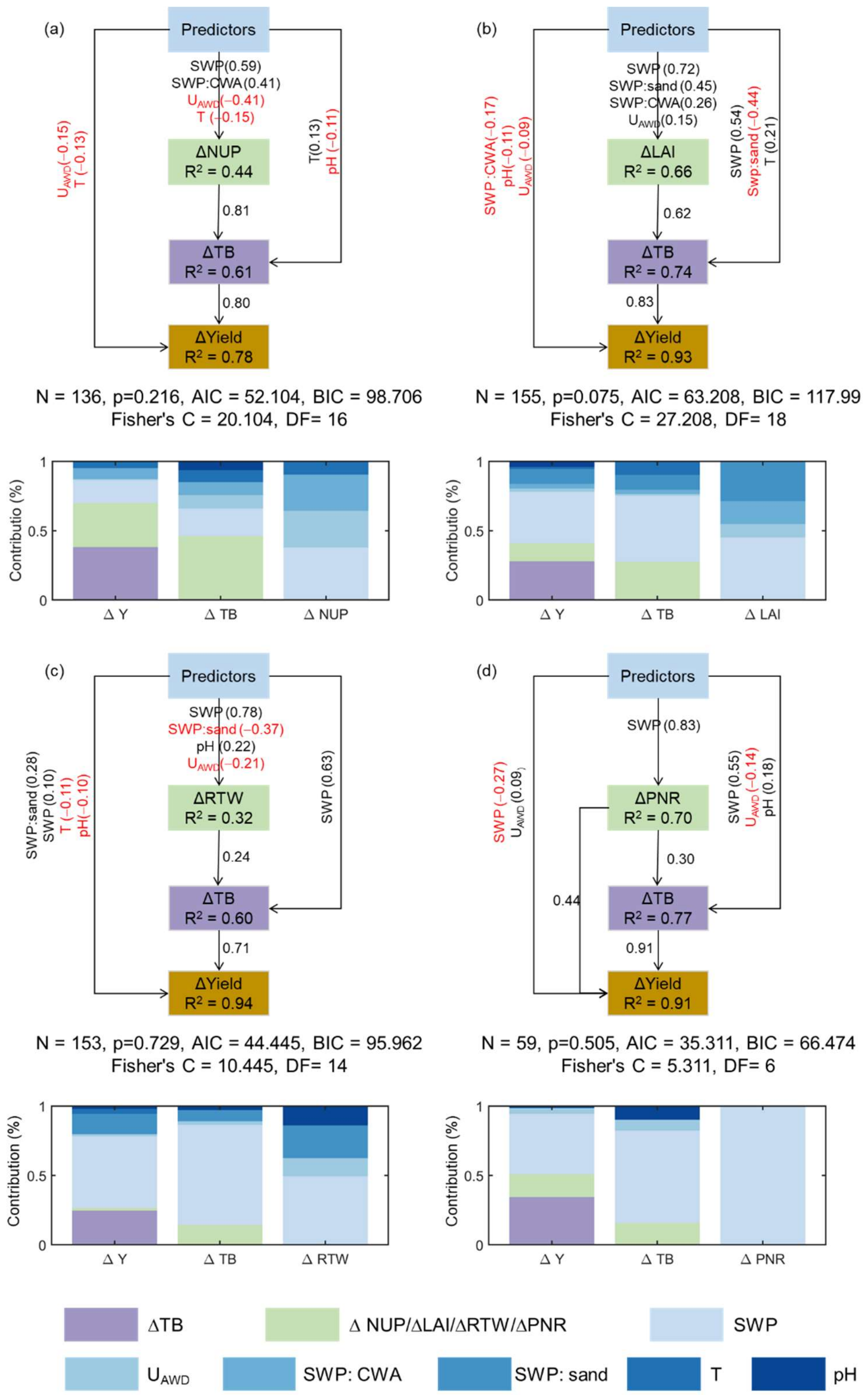

Fig. S11 Potential mechanisms underlying ΔY. Structural equation models show effects of physiological traits and predictors on ΔY and their relative contributions. Values next to arrows were standardized path coefficients for corrresponding predictors, interpreted as the changes in the dependent variable when the independent variable changes by one standard deviation. The relative contribution of each predictor was calculated based on the absolute value of standardized total effects (sum of direct plus indirect effects).

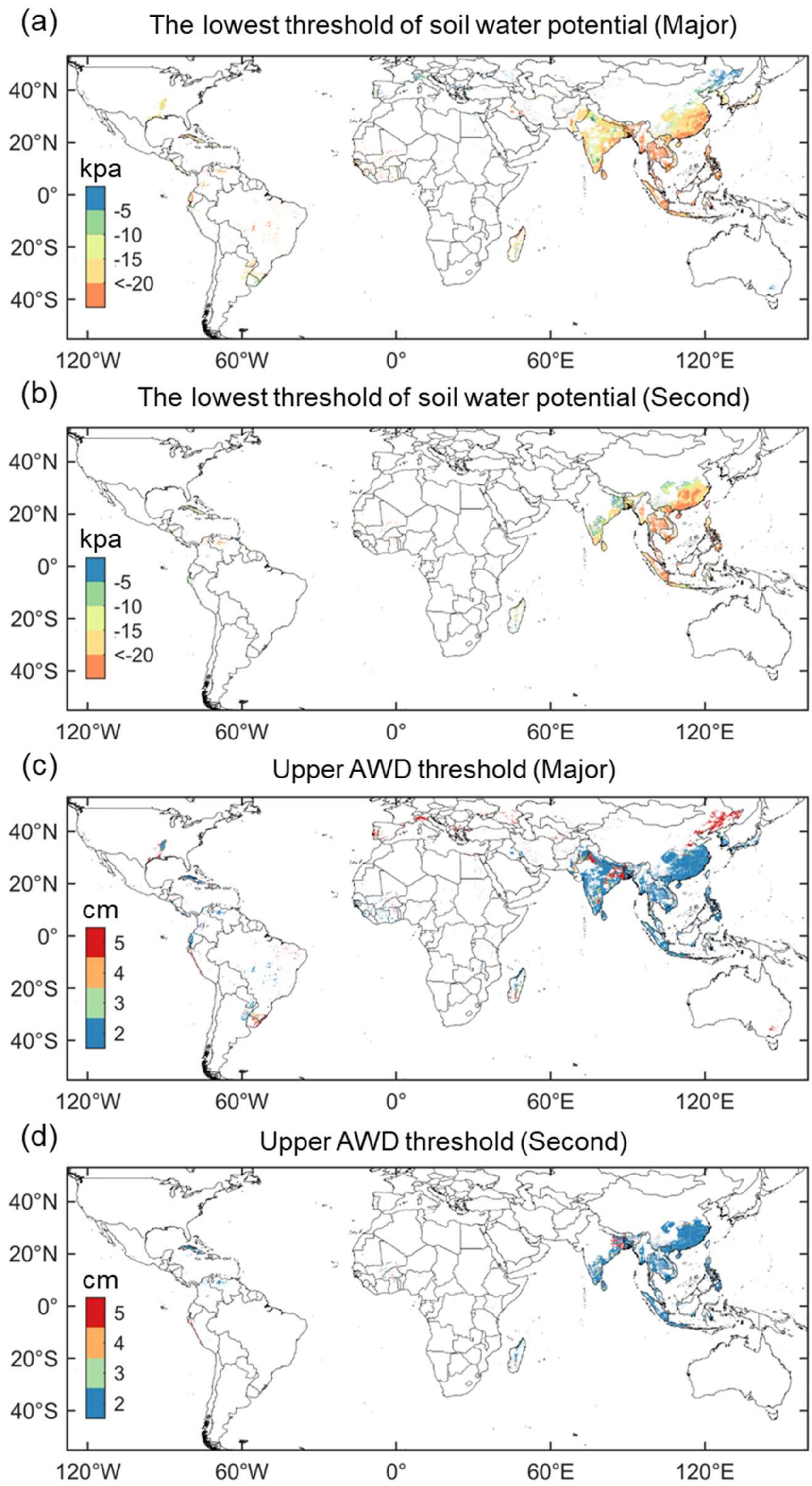

Fig. S12 Spatial pattern of the lowest (a-b) and upper (c-d) threshold of soil water potential-based AWD for the major and second rice growing season. Values are only shown where the proportion of irrigated harvested area within the grid cell is greater than 0.5%. Base map of the country boundaries was obtained from Resource and Environmental Science Data Platform of China (https://www.resdc.cn/data.aspx?DATAID=205).

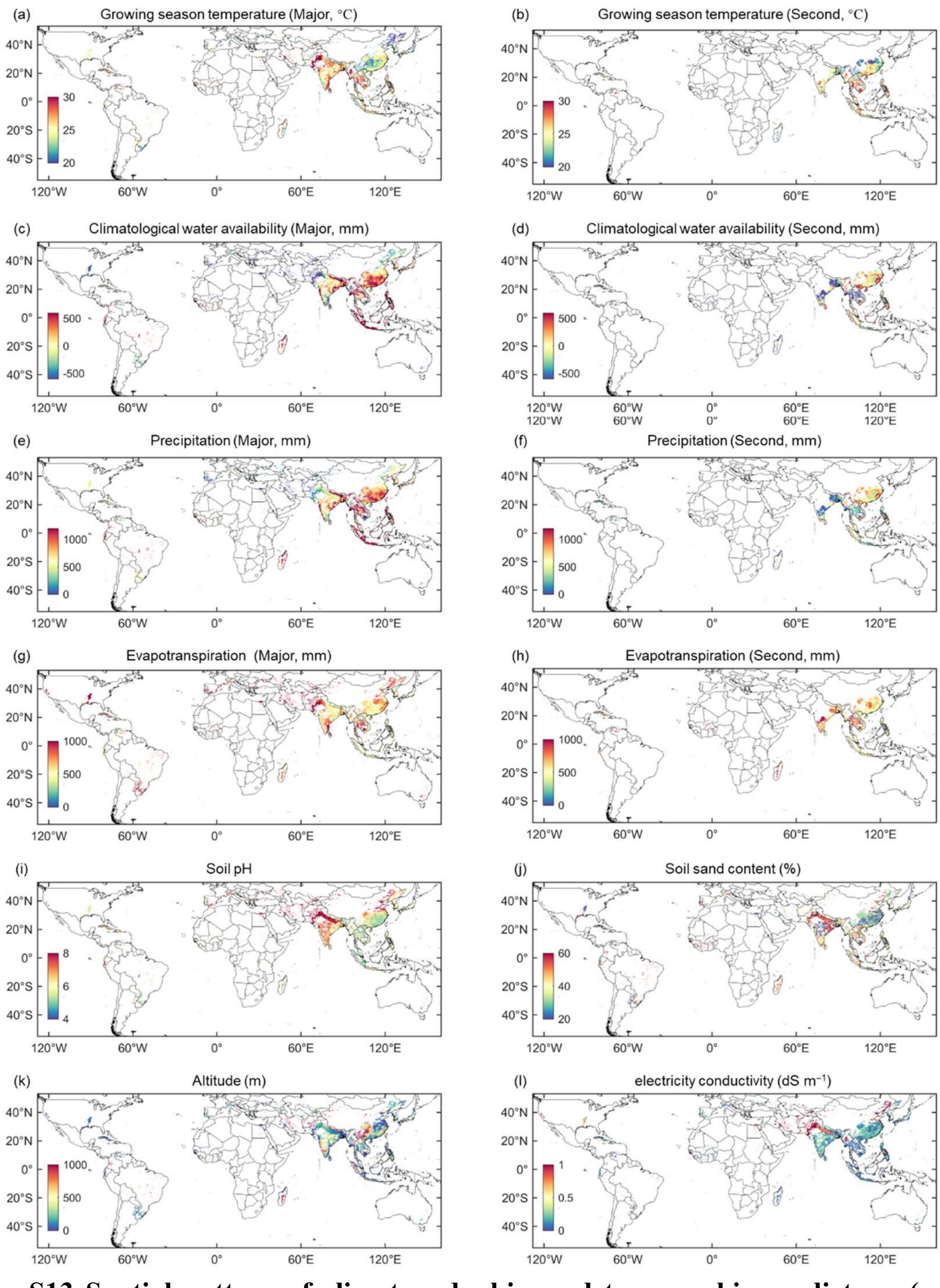

Fig. S13 Spatial pattern of climate, edaphic, and topographic predictors. (a-b) mean daily air temperature for the major and second rice growing season, **(c-d)** climatological water availability (cumulative growing season precipitation minus crop evapotranspiration) for the major and second rice growing season, **(e-f)** cumulative growing season precipitation for the major and second rice growing season, **(g-h)** cumulative crop evapotranspiration for the major and second rice growing season, **(i)** soil pH, **(j)** soil sand content, **(k)** altitude, and **(i)** soil electricity conductivity (indicating soil salinity). Base map of the country boundaries was obtained from Resource and Environmental Science Data Platform of China (https://www.resdc.cn/data.aspx?DATAID=205).

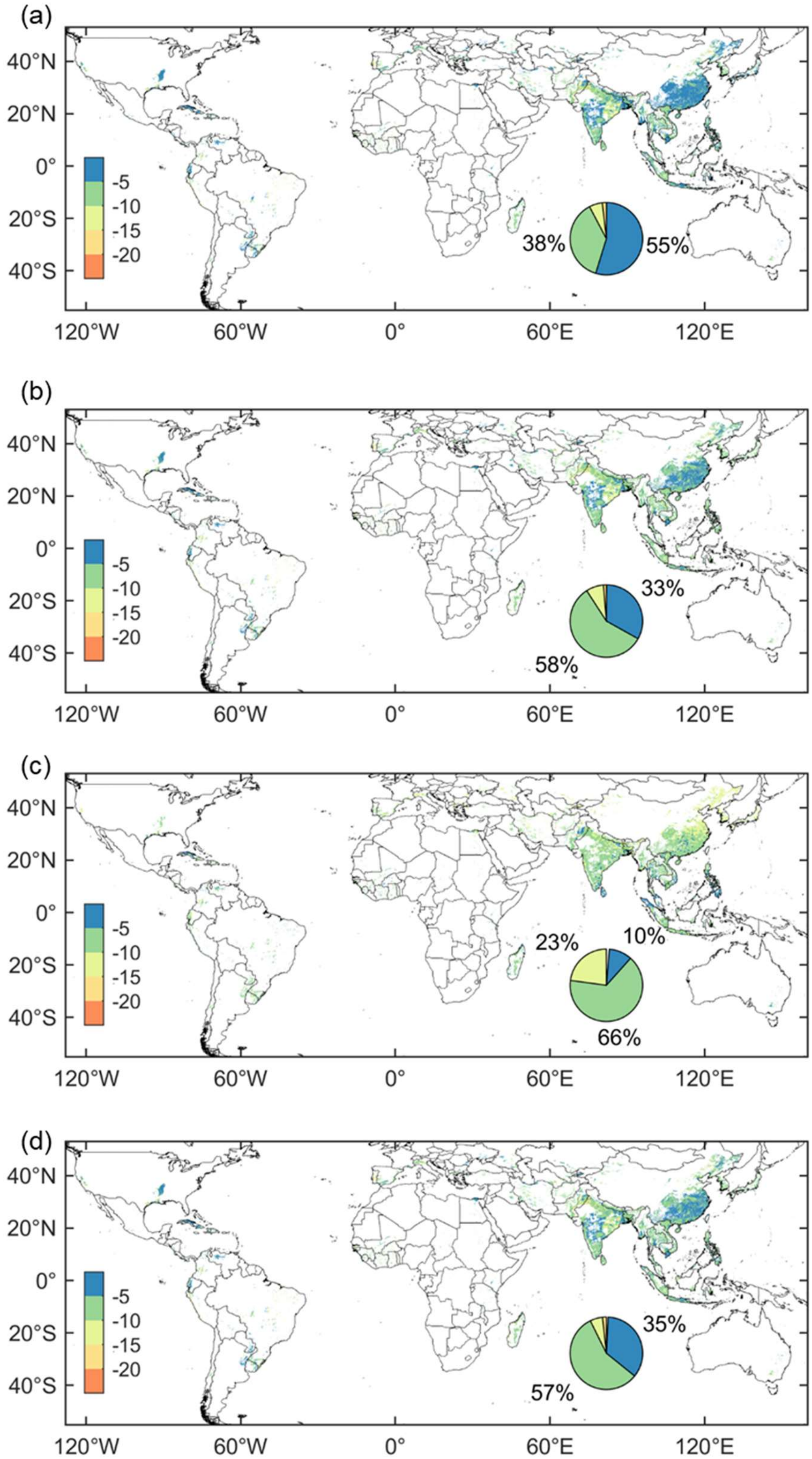

Fig. S14 Spatial pattern of predicted soil water potential at field water depth of −15cm based on three approaches and their median (kpa). Estimates based on **(a)** power function, **(b)** exponential function, **(c)** the processed-based WHCNS model and **(d)** median value of three approaches. Base map of the country boundaries was obtained from Resource and Environmental Science Data Platform of China (https://www.resdc.cn/data.aspx?DATAID=205).

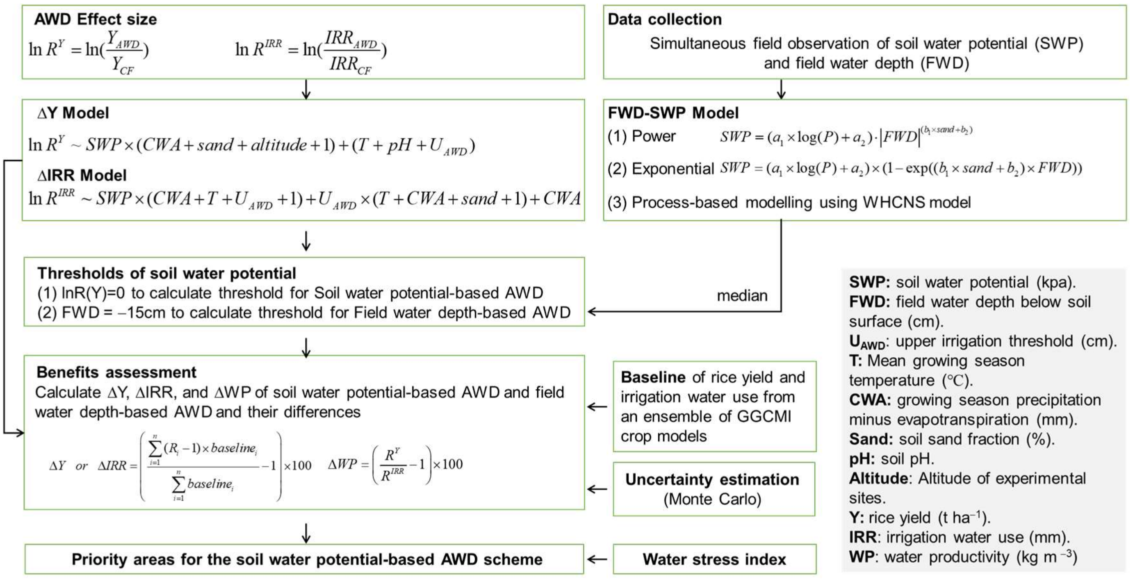

Fig. S15 Methodology flowchart of this study.

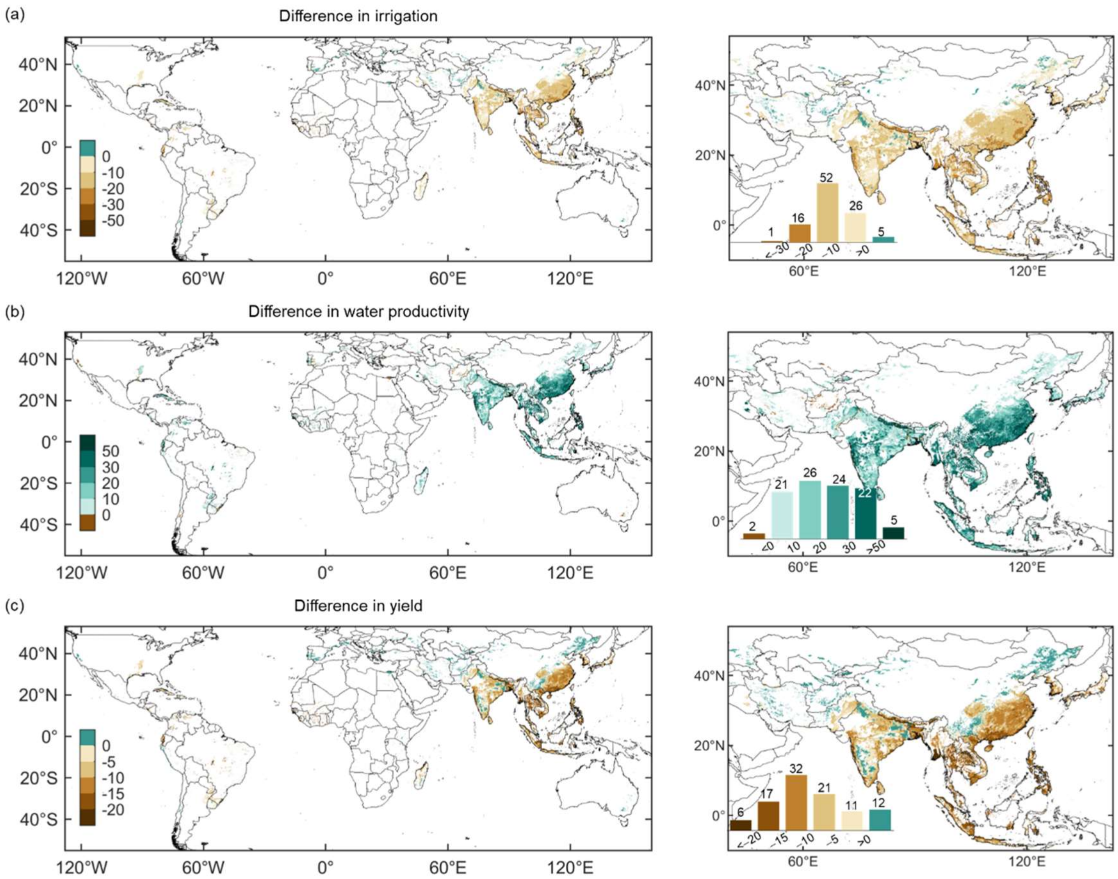

Fig. S16 Spatial pattern of differences in AWD-induced changes in (a) irrigation water use, (b) water productivity and (c) rice yield between soil water potential-based and field water depth-based AWD schemes (%). The inset bar plot represents the percentage (%) of irrigated harvested rice areas that fall within the specified classification categories. Base map of the country boundaries was obtained from Resource and Environmental Science Data Platform of China (https://www.resdc.cn/data.aspx?DATAID=205).

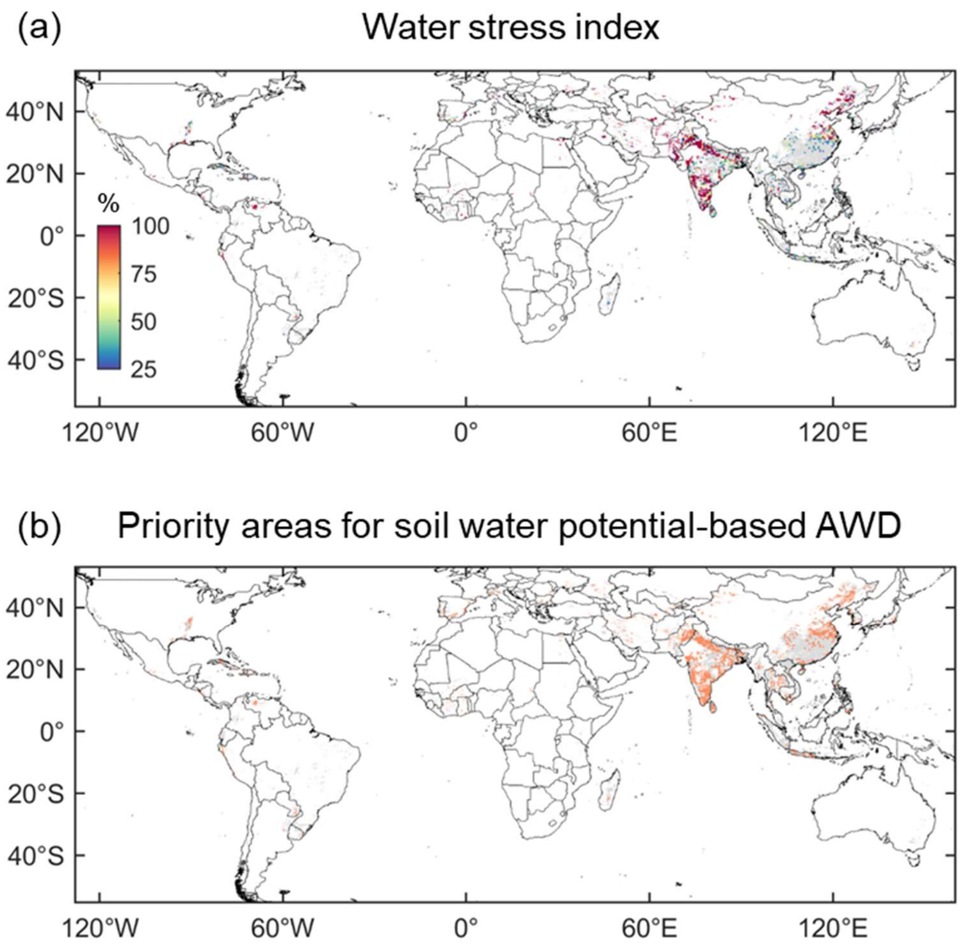

Fig. S17 Spatial pattern of (a) water stress index and (b) priority areas for the soil water potential-based AWD scheme. See Supplementary Text 3 for water-stressed regions identification. Base map of the country boundaries was obtained from Resource and Environmental Science Data Platform of China (https://www.resdc.cn/data.aspx?DATAID=205).

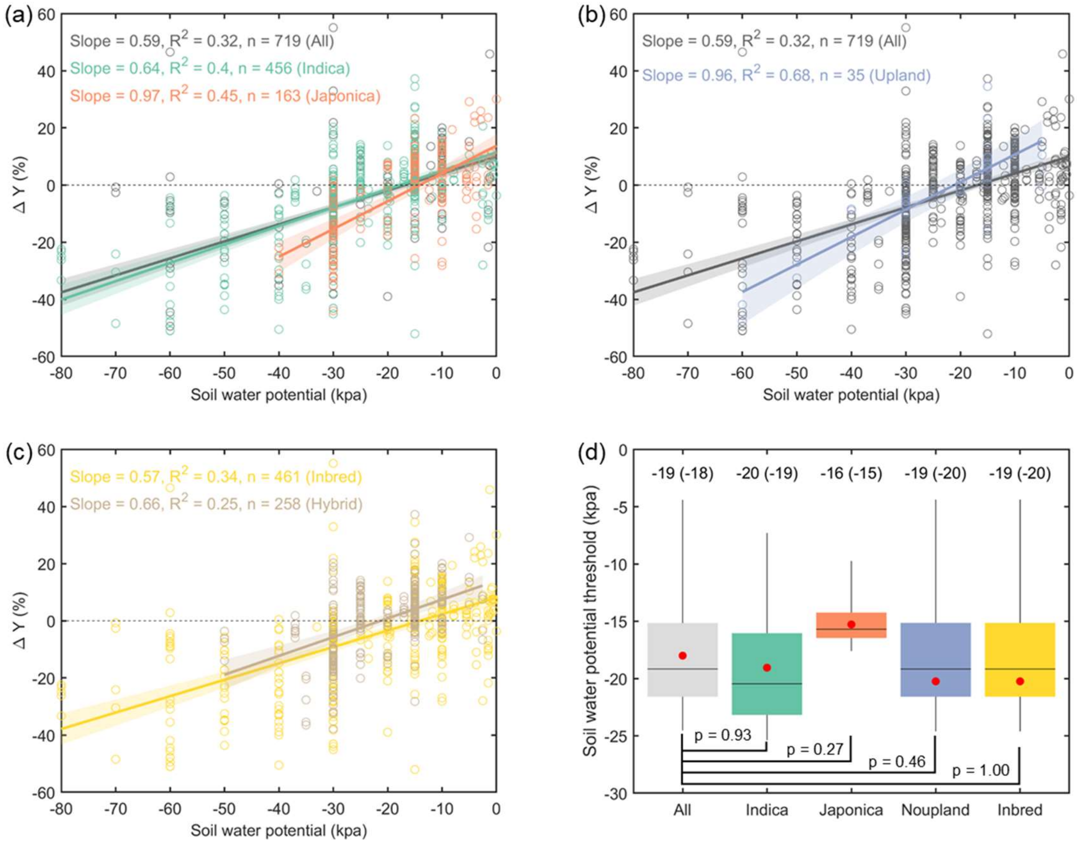

Fig. S18 Sensitivity test against rice cultivar. (a) Relationships between ΔY and the lowest soil water potential based on all observations (Grey), observations of Indica (Green) or Japonica rice (Orange). **(b)** Relationships between ΔY and the lowest soil water potential based on all observations (Grey) and observations of upland rice (Blue). **(c)** Relationships between ΔY and the lowest soil water potential based on observations of Inbred (Yellow) or Hybrid rice (Brown). The lines in **a-c** are regression lines ($P < 0.05$ based on two-sided t-test) with shading areas around each line represents the 95% confidence interval. **(d)** Prediction of the lowest soil water potential thresholds (kpa) based on ΔY models calibrated with all observations, and subsets with observations of Indica (green), Japonica (Orange), paddy rice (i.e., excluding upland rice) (Blue) or Inbred rice (Yellow). The statistical significance in **(d)** was tested using two-sided Wilcoxon signed rank test, with n = 176,307 for global irrigated rice area grids at 5-arc-minute spatial resolution. The boxes and whiskers show the 5th, 25th, median, 75th and 95th percentiles and the red dots show the mean value of the data.

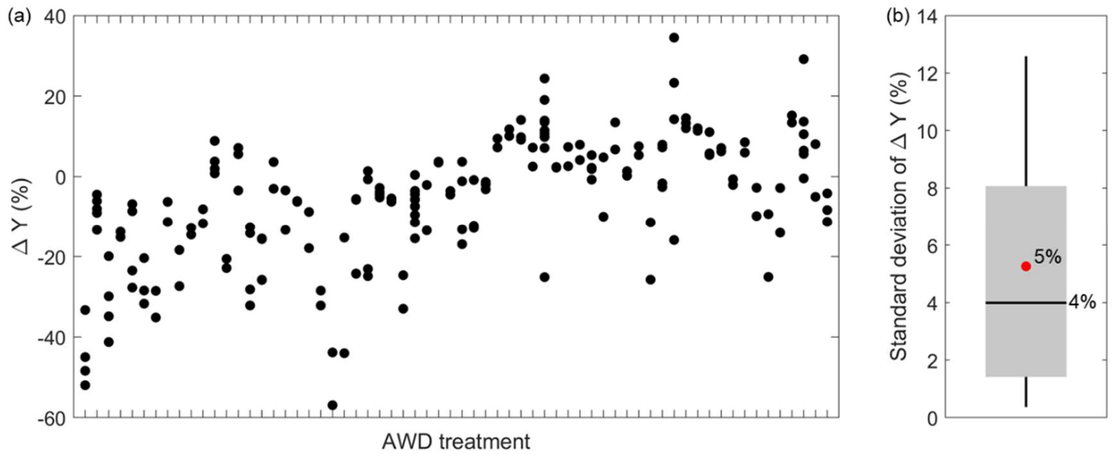

Fig. S19 Impact of rice cultivars on ΔY. **(a)** ΔY of different cultivars from the same AWD treatment. Each column represents the same AWD treatment from the same study. Points in the same column indicate ΔY of different cultivars under the same AWD treatment. Figure (a) shows 190 points from 64 AWD treatments of 37 studies. **(b)** Boxplot of standard deviation of ΔY caused by cultivar differences (*n* = 64). The boxes and whiskers show the 5th, 25th, median, 75th and 95th percentiles and the red dots show the mean value of the data.

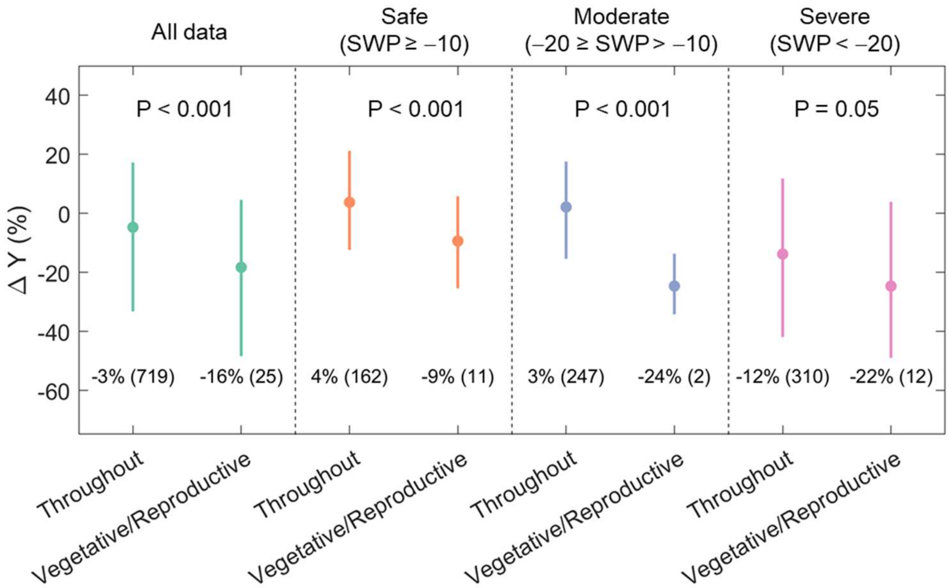

Fig. S20 Impact of AWD application timing on ΔY. This figure shows differences in ΔY between AWD applied throughout the entire season (Throughout) and only at vegetative or reproductive stage (Vegetative/Reproductive), based on all observations and observations of different levels of lower AWD thresholds. The significance was tested using two-sided Wilcoxon signed rank test. The vertical lines and the dots indicate the 5^{th} and 95^{th} percentile range and the mean value of ΔY. Numbers in the bottom indicate averaged ΔY and number of records.

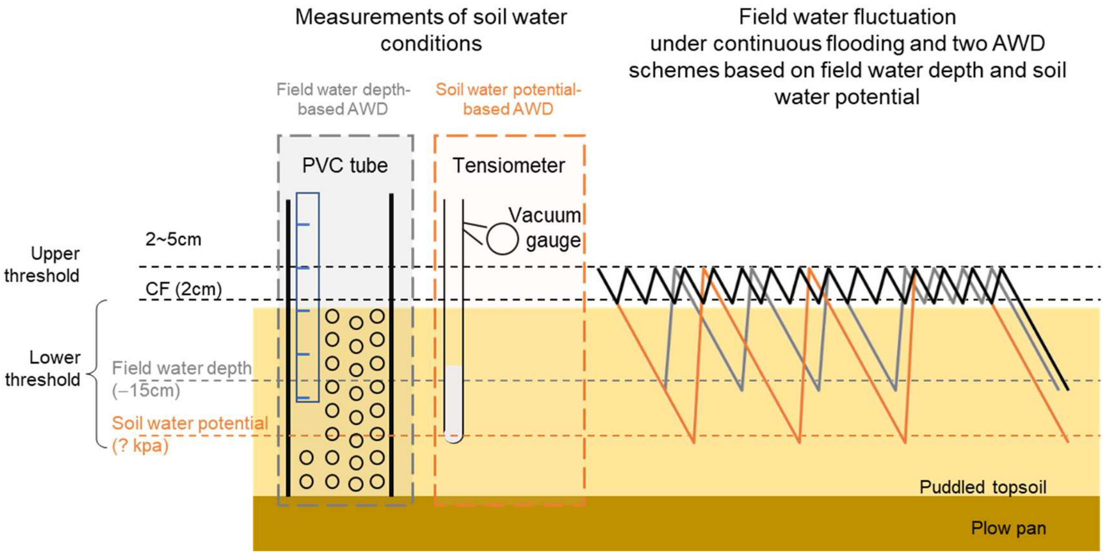

Fig. S21 Schematic representation of irrigation scheduling under continuous flooding (black), soil water potential-based AWD scheme (orange) and field water depth-based AWD scheme (gray). Left part shows the PVC tube and tensiometer used to monitor perched field water depth and soil water potential, respectively.

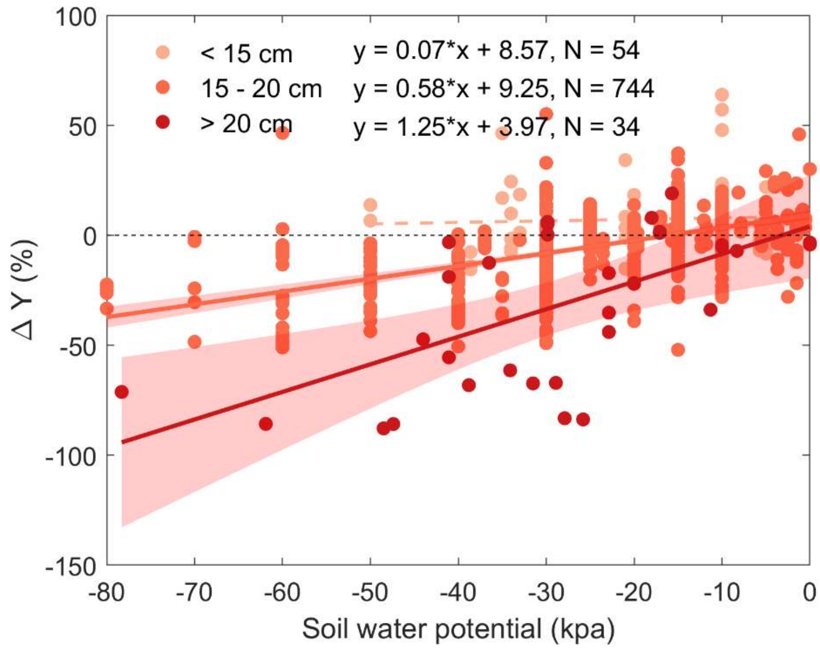

Fig. S22 Relationships between ΔY and the lowest soil water potential at different soil depths. The red lines are regression lines with dashed lines indicating non-significant relationship (P > 0.05) based on two-sided t-test. The range of the error bands shows the 95% confidence intervals of the estimations of the regression model.

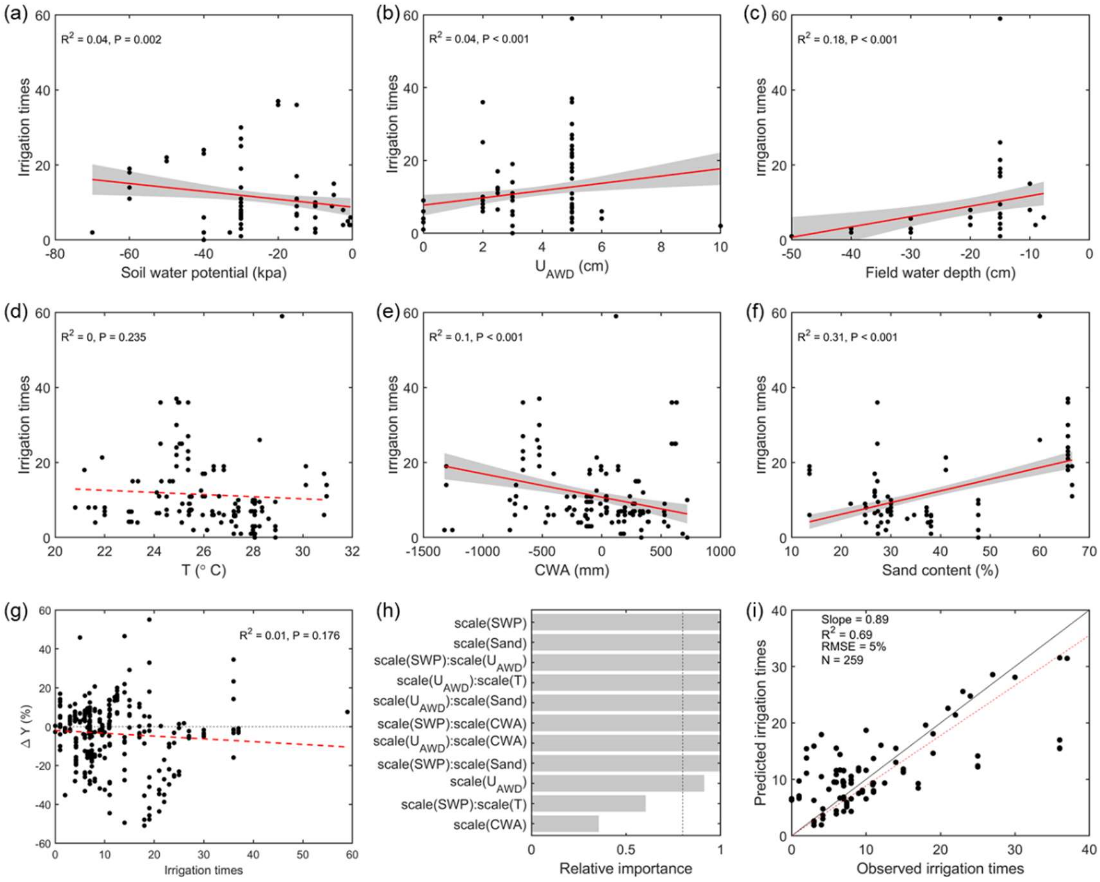

Fig. S23 Impact factors of AWD cycles (irrigation times). (a-f) Relationships between irrigation times and **(a)** soil water potential, **(b)** upper irrigation threshold, **(c)** field water depth, **(d)** mean growing season temperature, **(e)** climatological water availability, **(f)** soil sand content. **(g)** Relationships between ΔY and irrigation times. **(h)** Relative importance of potential predictors for explaining variations in irrigation times. The importance is based on the sum of the Akaike weights derived from model selection using corrected Akaike information criterion. The cutoff is set at 0.8 to differentiate among the most important predictors. **(i)** Model performance for simulating irrigation times based on linear regression using the important predictors in (h). Red lines in all figures are regression lines with dashed lines indicating non-significant relationships (P > 0.05) based on two-sided t-test. Gray shading around each line represents the 95% confidence interval.

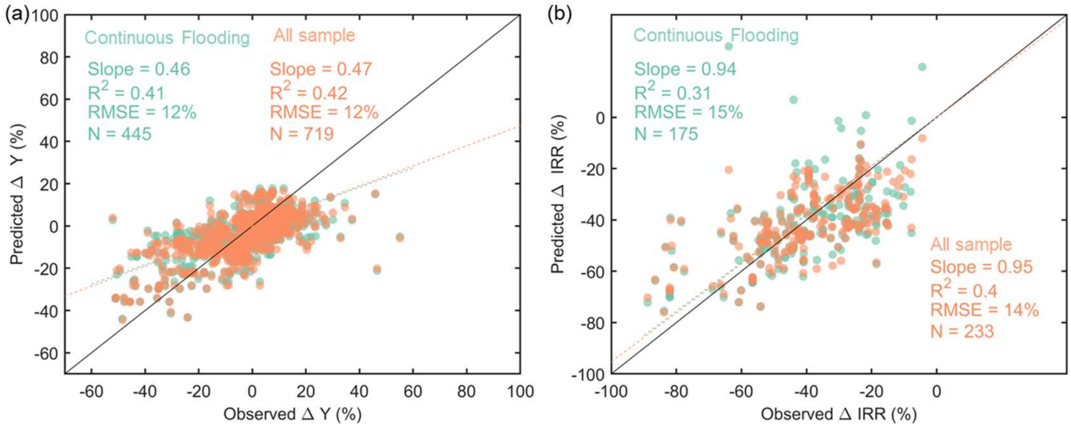

Fig. S24 Sensitivity test against irrigation method in the control group. Predicted ΔY **(a)** and ΔIRR **(b)** based on observations with irrigation method in control group including only continuous flooding (green) or both continuous flooding and a mid-season drainage (orange).

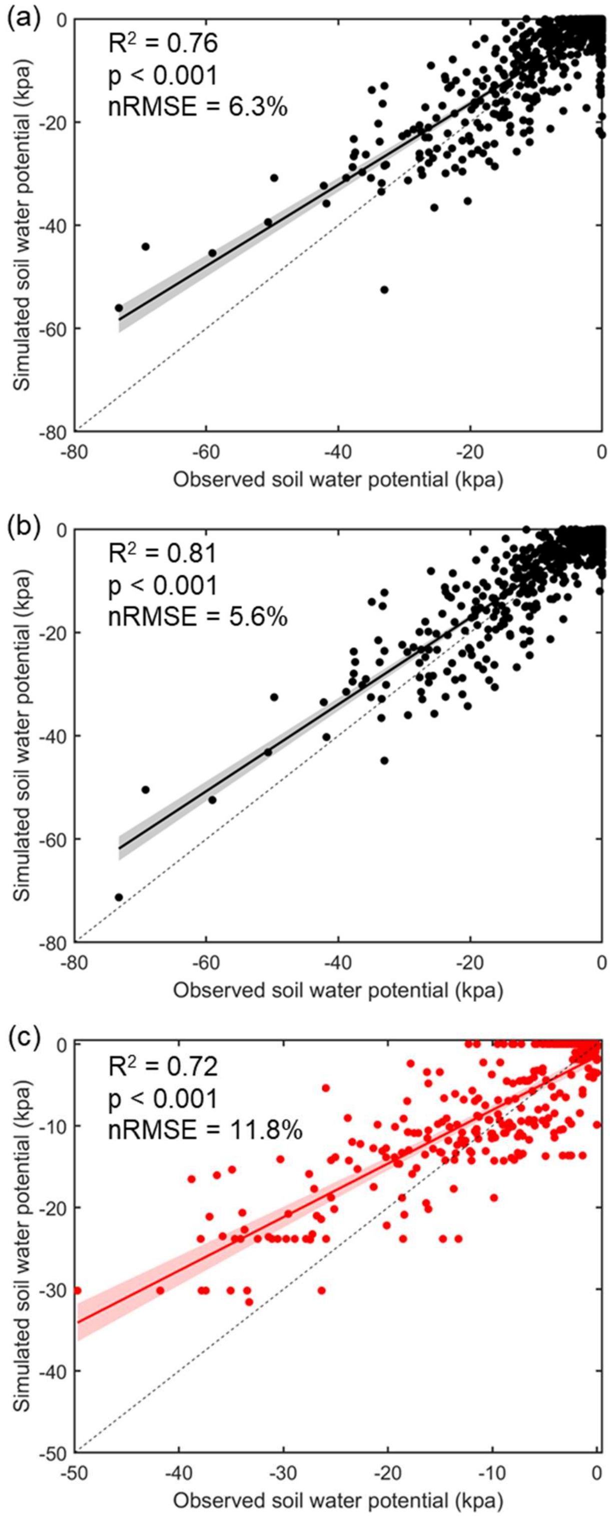

Fig. S25 Model performance for quantifying relationships between field water depth and soil water potential. Model performance based on **(a)** statistical model of power function, **(b)** statistical model of exponential function, and **(c)** process-based model (WHCNS). The solid lines are regression lines with shading areas around each line represents the 95% confidence interval based on two-sided t-test. The dashed black lines are 1:1 lines.

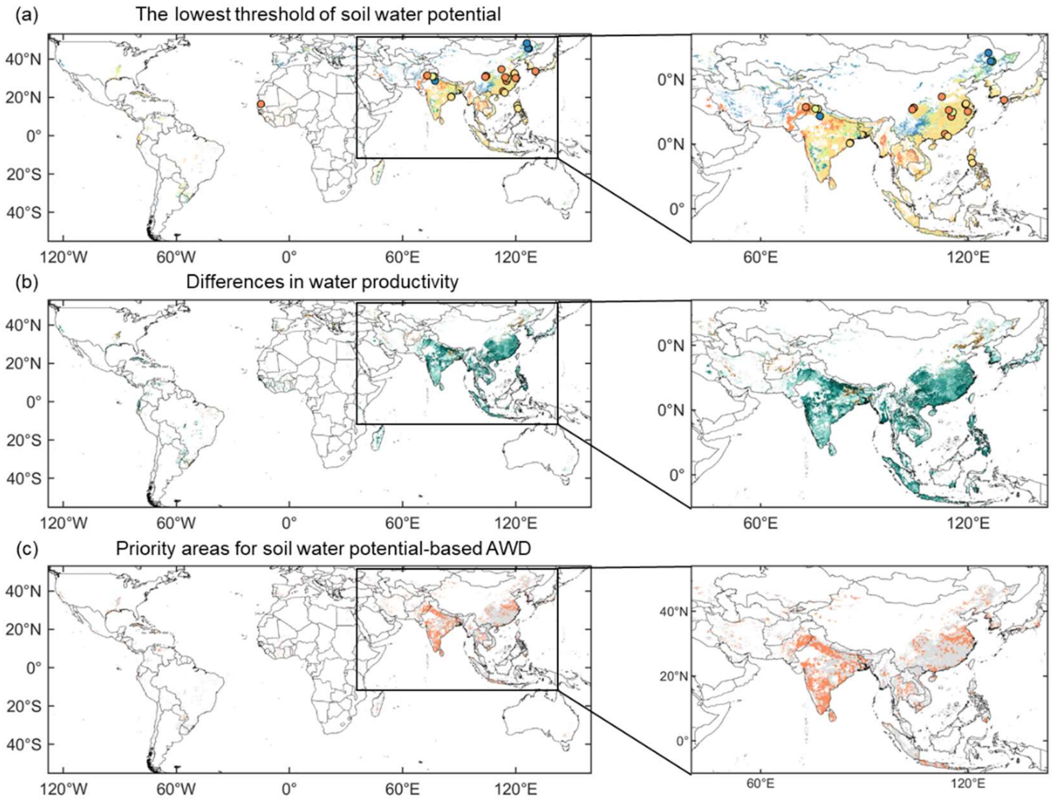

Fig. S26 Results based on soil data from the Harmonized World Soil Database. **(a)** The lowest threshold of soil water potential (kpa). **(b)** Differences in water productivity (%). **(c)** Priority areas for the soil water potential-based AWD scheme. The left column presents global view and the right column shows enlarged maps for South, East and Southeast Asia. Base map of the country boundaries was obtained from Resource and Environmental Science Data Platform of China (https://www.resdc.cn/data.aspx?DATAID=205).

$$SWP = a \cdot |FWL|^b$$

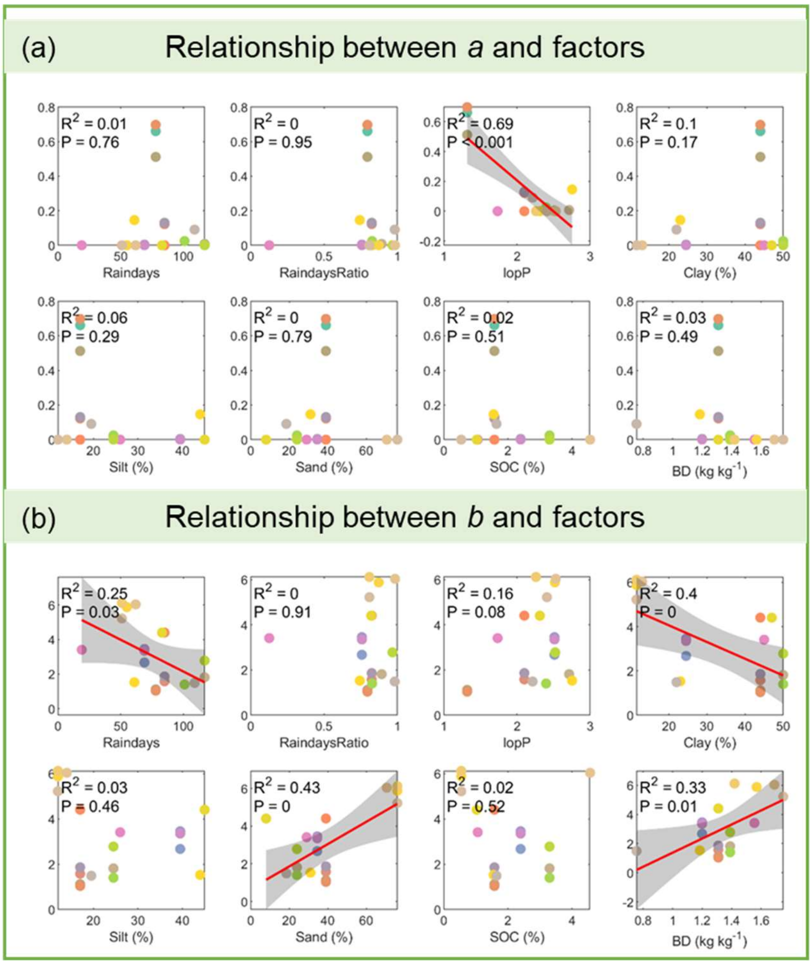

Fig. S27 Relationships between environmental factors and parameters of the power function empirical model quantifying relationships between field water depth and soil water potential. Red lines are fitting lines and grey area indicates 95% confidence interval, shown only for significant regression relationships (P < 0.05) based on two-sided t-test. *Raindays* indicates total number of days with precipitation during growing season. *RaindaysRatio* indicates ratio of rainy days to total days of growing season. *logP* indicates log-transformed growing season precipitation. *Clay*, *Silt*, and *Sand* indicate soil clay, silt and sand contents. *SOC* indicates soil organic carbon. *BD* indicates soil bulk density.

$$SWP = a \times (1 - \exp(b \times FWL))$$

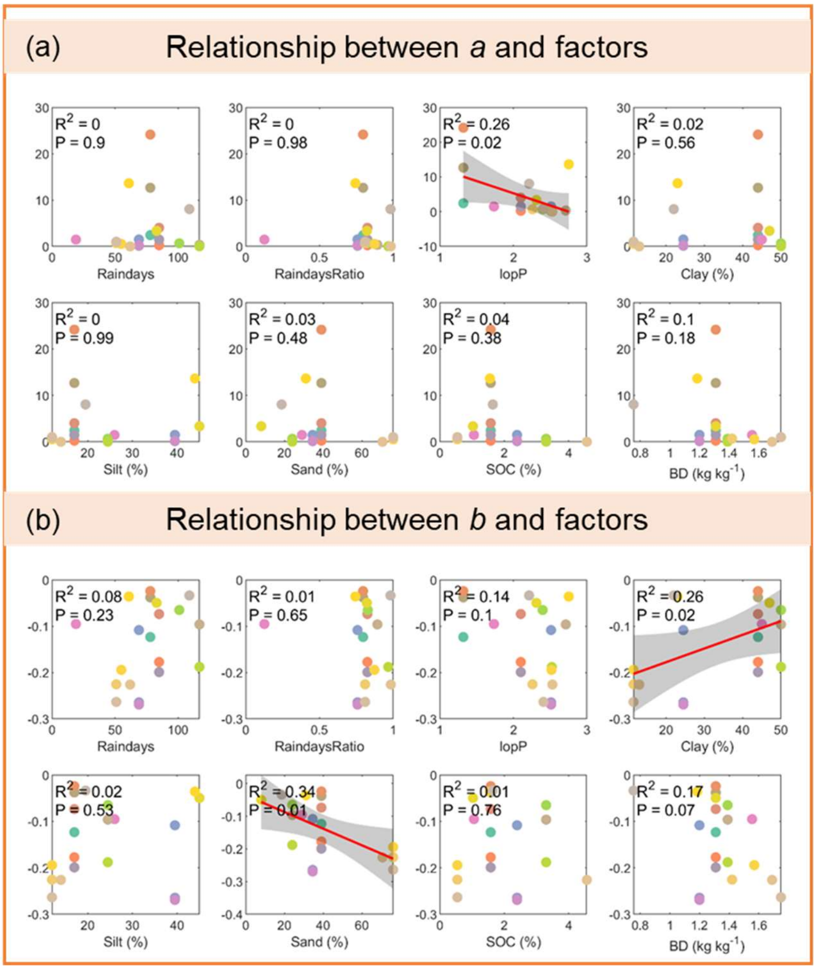

Fig. S28 Same with Fig. S27, but based on exponential function empirical model.

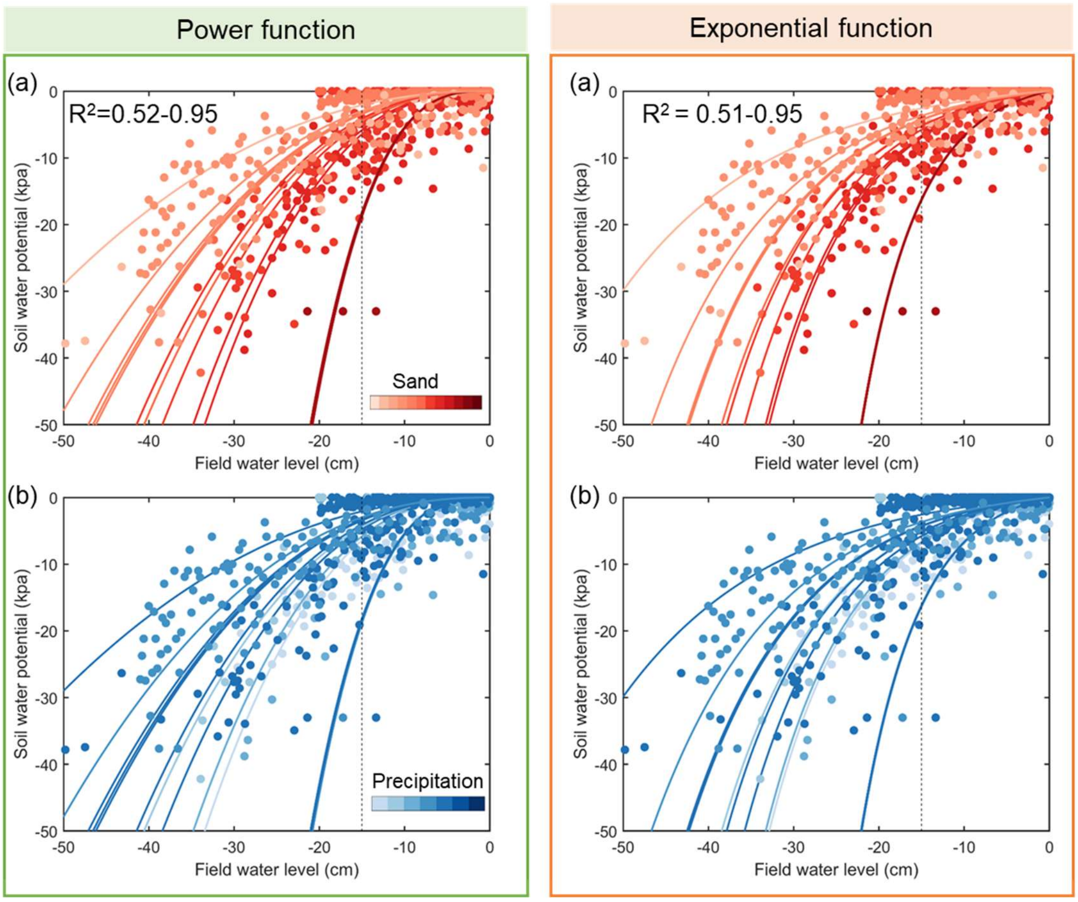

Fig. S29 Observed and predicted relationships between field water depth and soil water potential in different levels of soil sand fraction and precipitation based on empirical model of power (left panel) and exponential function (right panel).

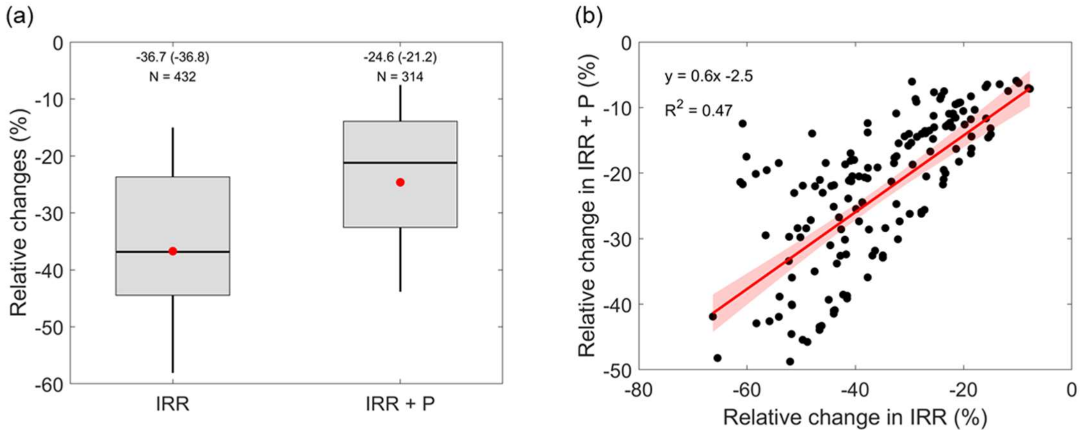

Fig. S30 AWD effects on irrigation water use and total water input. (a) AWD effects on irrigation water use (IRR) and total water input from irrigation and precipitation (IRR+P). The boxes and whiskers show the 5th, 25th, median, 75th and 95th percentiles and the red dots show the mean value of the data. The numbers indicate mean and median value of relative changes and number of observations. **(b)** Relationships between relative changes in irrigation water use and total water input. The red line is the regression line ($P < 0.001$ based on two-sided t-test) with the shading around representing the 95% confidence interval.

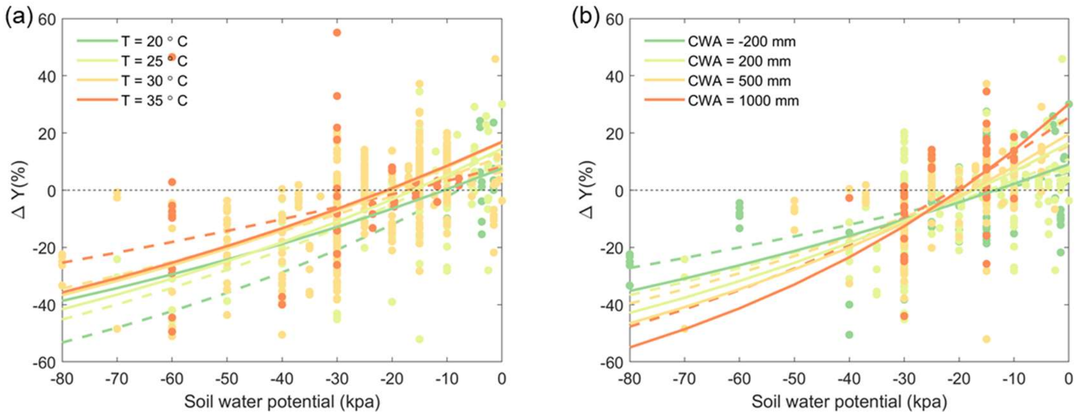

Fig. S31 Predicted ΔY in response to soil water potential thresholds under different levels of (a) mean growing season temperature and (b) climatological water availability. Solid lines are fitted lines of predictions from the ΔY model (Equation 1 in the main text), with the other predictors set as their mean value of observations. Dashed lines are regression lines between ΔY and soil water potential based on observations in corresponding classification. Noted that ln-transformed ΔY was used as dependent variable in the regression, and then transformed back to percentage changes based on predictions.

Reference

1. Yang JC, Zhou Q, Zhang JH. Moderate wetting and drying increases rice yield and reduces water use, grain arsenic level, and methane emission. *Crop J* **5**, 151-158 (2017).
2. Carrijo DR, Lundy ME, Linquist BA. Rice yields and water use under alternate wetting and drying irrigation: A meta-analysis. *Field Crop Res* **203**, 173-180 (2017).
3. Liang H, Yang S, Xu J, Hu K. Modeling water consumption, N fates, and rice yield for water-saving and conventional rice production systems. *Soil and Tillage Research* **209**, 104944 (2021).
4. Takeda N*, et al.* Estimating Soil Water Contents from Field Water Tables for Potential Rice Irrigation Criteria under Contour-Levee Irrigation Systems. *Environment Control in Biology* **57**, 15-21 (2019).
5. Liang K*, et al.* Grain yield, water productivity and CH4 emission of irrigated rice in response to water management in south China. *Agr Water Manage* **163**, 319-331 (2016).
6. Novick KA*, et al.* Confronting the water potential information gap. *Nat Geosci* **15**, 158-164 (2022).
7. Allan R, Pereira L, Smith M. *Crop evapotranspiration-Guidelines for computing crop water requirements-FAO Irrigation and drainage paper 56* (1998).
8. Hachum Ahmed Y, Alfaro Jose F. Rain Infiltration into Layered Soils: Prediction. *Journal of the Irrigation and Drainage Division* **106**, 311-319 (1980).
9. van Genuchten MT. A Closed-form Equation for Predicting the Hydraulic Conductivity of Unsaturated Soils. *Soil Science Society of America Journal* **44**, 892-898 (1980).
10. Hersbach, H., Bell, B., Berrisford, P., Biavati, G., Horányi, A., Muñoz Sabater, J., Nicolas, J., Peubey, C., Radu, R., Rozum, I., Schepers, D., Simmons, A., Soci, C., Dee, D., Thépaut, J.-N. (2018) ERA5 hourly data on single levels from 1979 to present. Copernicus Climate Change Service (C3S) Climate Data Store (CDS). (Accessed on < 06-10-2021>), 10.24381/cds.adbb2d47.
11. Han, Eunjin; Ines, Amor; Koo, Jawoo, 2015, "Global High-Resolution Soil Profile Database for Crop Modeling Applications", http://dx.doi.org/10.7910/DVN/1PEEY0, Harvard Dataverse, V1.
12. Lampayan RM, Rejesus RM, Singleton GR, Bouman BAM. Adoption and economics of alternate wetting and drying water management for irrigated lowland rice. *Field Crop Res* **170**, 95-108 (2015).
13. FAO and UN Water. 2021. Progress on Level of Water Stress. Global status and acceleration needs for SDG Indicator 6.4.2, 2021. Rome. https://doi.org/10.4060/cb6241en.
14. Veldkamp TIE*, et al.* Water scarcity hotspots travel downstream due to human interventions in the 20th and 21st century. *Nature Communications* **8**, 15697 (2017).

15. Zhang Y*, et al.* Integrated management approaches enabling sustainable rice production under alternate wetting and drying irrigation. *Agr Water Manage* **281**, 108265 (2023).
16. Cheng HM*, et al.* Effects of alternate wetting and drying irrigation on yield, water and nitrogen use, and greenhouse gas emissions in rice paddy fields. *J Clean Prod* **349**, 131487 (2022).
17. Ishfaq M*, et al.* Alternate wetting and drying: A water-saving and ecofriendly rice production system. *Agr Water Manage* **241**, 106363 (2020).
18. Jiang Y*, et al.* Water management to mitigate the global warming potential of rice systems: A global meta-analysis. *Field Crop Res* **234**, 47-54 (2019).
19. Hanasaki N*, et al.* An integrated model for the assessment of global water resources Part 1: Model description and input meteorological forcing. *Hydrol Earth Syst Sc* **12**, 1007-1025 (2008).
20. Hanasaki N*, et al.* An integrated model for the assessment of global water resources Part 2: Applications and assessments. *Hydrol Earth Syst Sc* **12**, 1027-1037 (2008).
21. Bondeau A*, et al.* Modelling the role of agriculture for the 20th century global terrestrial carbon balance. *Global Change Biol* **13**, 679-706 (2007).
22. Schaphoff S, Heyder U, Ostberg S, Gerten D, Heinke J, Lucht W. Contribution of permafrost soils to the global carbon budget. *Environ Res Lett* **8**, (2013).
23. Pokhrel YN*, et al.* Incorporation of groundwater pumping in a global Land Surface Model with the representation of human impacts. *Water Resour Res* **51**, 78-96 (2015).
24. van Beek LPH, Wada Y, Bierkens MFP. Global monthly water stress: 1. Water balance and water availability. *Water Resour Res* **47**, (2011).
25. Wada Y, Wisser D, Bierkens MFP. Global modeling of withdrawal, allocation and consumptive use of surface water and groundwater resources. *Earth Syst Dynam* **5**, 15-40 (2014).
26. Zhang H, Xue Y, Wang Z, Yang J, Zhang J. An Alternate Wetting and Moderate Soil Drying Regime Improves Root and Shoot Growth in Rice. *Crop Science* **49**, 2246-2260 (2009).
27. Zhang H*, et al.* Alternative fertilizer and irrigation practices improve rice yield and resource use efficiency by regulating source-sink relationships. *Field Crop Res* **265**, 108124 (2021).
28. Yang C, Yang L, Yang Y, Ouyang Z. Rice root growth and nutrient uptake as influenced by organic manure in continuously and alternately flooded paddy soils. *Agr Water Manage* **70**, 67-81 (2004).
29. Yang JC, Zhang JH. Crop management techniques to enhance harvest index in rice. *J Exp Bot* **61**, 3177-3189 (2010).
30. Ouyang W, Yin X, Yang J, Struik PC. Roles of canopy architecture and nitrogen distribution in the better performance of an aerobic than a lowland rice cultivar under water deficit. *Field Crop Res* **271**, 108257 (2021).
31. Zhong C, Jian SF, Huang J, Jin QY, Cao XC. Trade-off of within-leaf nitrogen allocation between photosynthetic nitrogen-use efficiency and water deficit

stress acclimation in rice (Oryza sativa L.). *Plant Physiol Bioch* **135**, 41-50 (2019).

32. Zhang H, Zhang S, Yang J, Zhang J, Wang Z. Postanthesis Moderate Wetting Drying Improves Both Quality and Quantity of Rice Yield. *Agronomy Journal* **100**, 726-734 (2008).
33. Singh Y*, et al.* Crop performance in permanent raised bed rice–wheat cropping system in Punjab, India. *Field Crop Res* **110**, 1-20 (2009).
34. Cabangon RJ, Castillo EG, Tuong TP. Chlorophyll meter-based nitrogen management of rice grown under alternate wetting and drying irrigation. *Field Crop Res* **121**, 136-146 (2011).
35. Chidthaisong A*, et al.* Evaluating the effects of alternate wetting and drying (AWD) on methane and nitrous oxide emissions from a paddy field in Thailand. *Soil Sci Plant Nutr* **64**, 31-38 (2018).
36. Setyanto P*, et al.* Alternate wetting and drying reduces methane emission from a rice paddy in Central Java, Indonesia without yield loss. *Soil Sci Plant Nutr* **64**, 23-30 (2018).
37. Setyanto P, Bakar RA. METHANE EMISSION FROM PADDY FIELDS AS INFLUENCED BY DIFFERENT WATER REGIMES IN CENTRAL JAVA. *Indonesian Journal of Agricultural Science* **6**, 1-9 (2005).
38. de Vries ME, Rodenburg J, Bado BV, Sow A, Leffelaar PA, Giller KE. Rice production with less irrigation water is possible in a Sahelian environment. *Field Crop Res* **116**, 154-164 (2010).
39. Zheng J*, et al.* Effect of zeolite application on phenology, grain yield and grain quality in rice under water stress. *Agr Water Manage* **206**, 241-251 (2018).
40. Zheng J, Chen T, Xia G, Chen W, Liu G, Chi D. Effects of zeolite application on grain yield, water use and nitrogen uptake of rice under alternate wetting and drying irrigation. *International Journal of Agricultural and Biological Engineering* **11**, 157-164 (2018).
41. Li Y*, et al.* Zeolite increases paddy soil potassium fixation, partial factor productivity, and potassium balance under alternate wetting and drying irrigation. *Agr Water Manage* **260**, 107294 (2022).
42. Belder P*, et al.* Effect of water-saving irrigation on rice yield and water use in typical lowland conditions in Asia. *Agr Water Manage* **65**, 193-210 (2004).
43. Devkota KP*, et al.* Growth and yield of rice (Oryza sativa L.) under resource conservation technologies in the irrigated drylands of Central Asia. *Field Crop Res* **149**, 115-126 (2013).
44. Howell KR, Shrestha P, Dodd IC. Alternate wetting and drying irrigation maintained rice yields despite half the irrigation volume, but is currently unlikely to be adopted by smallholder lowland rice farmers in Nepal. *Food and Energy Security* **4**, 144-157 (2015).

PRISMA 2020 Checklist

Section and Topic	Item #	Checklist item	Location where item is reported
TITLE			
Title	1	Identify the report as a systematic review.	Title page
ABSTRACT			
Abstract	2	See the PRISMA 2020 for Abstracts checklist.	Abstract section, Lines 28-41
INTRODUCTION			
Rationale	3	Describe the rationale for the review in the context of existing knowledge.	Lines 45-71
Objectives	4	Provide an explicit statement of the objective(s) or question(s) the review addresses.	Lines 73-81
METHODS			
Eligibility criteria	5	Specify the inclusion and exclusion criteria for the review and how studies were grouped for the syntheses.	Lines 296-310
Information sources	6	Specify all databases, registers, websites, organisations, reference lists and other sources searched or consulted to identify studies. Specify the date when each source was last searched or consulted.	Lines 296-300
Search strategy	7	Present the full search strategies for all databases, registers and websites, including any filters and limits used.	NA
Selection process	8	Specify the methods used to decide whether a study met the inclusion criteria of the review, including how many reviewers screened each record and each report retrieved, whether they worked independently, and if applicable, details of automation tools used in the process.	Lines 296-316
Data collection process	9	Specify the methods used to collect data from reports, including how many reviewers collected data from each report, whether they worked independently, any processes for obtaining or confirming data from study investigators, and if applicable, details of automation tools used in the process.	Lines 296-300
Data items	10a	List and define all outcomes for which data were sought. Specify whether all results that were compatible with each outcome domain in each study were sought (e.g. for all measures, time points, analyses), and if not, the methods used to decide which results to collect.	Lines 296-316
	10b	List and define all other variables for which data were sought (e.g. participant and intervention characteristics, funding sources). Describe any assumptions made about any missing or unclear information.	Lines 318-343
Study risk of bias assessment	11	Specify the methods used to assess risk of bias in the included studies, including details of the tool(s) used, how many reviewers assessed each study and whether they worked independently, and if applicable, details of automation tools used in the process.	NA
Effect measures	12	Specify for each outcome the effect measure(s) (e.g. risk ratio, mean difference) used in the synthesis or presentation of results.	Lines 318-322
Synthesis methods	13a	Describe the processes used to decide which studies were eligible for each synthesis (e.g. tabulating the study intervention characteristics and comparing against the planned groups for each synthesis (item #5)).	Lines 350-357
	13b	Describe any methods required to prepare the data for presentation or synthesis, such as handling of missing summary statistics, or data conversions.	Lines 357-360, 402-405
	13c	Describe any methods used to tabulate or visually display results of individual studies and syntheses.	NA
	13d	Describe any methods used to synthesize results and provide a rationale for the choice(s). If meta-analysis was performed, describe the model(s), method(s) to identify the presence and extent of statistical heterogeneity, and software package(s) used.	Lines 357-372
	13e	Describe any methods used to explore possible causes of heterogeneity among study results (e.g. subgroup analysis, meta-regression).	NA
	13f	Describe any sensitivity analyses conducted to assess robustness of the synthesized results.	Lines 322-327, 370-371, 462-464

PRISMA 2020 Checklist

Section and Topic	Item #	Checklist item	Location where item is reported
Reporting bias assessment	14	Describe any methods used to assess risk of bias due to missing results in a synthesis (arising from reporting biases).	NA
Certainty assessment	15	Describe any methods used to assess certainty (or confidence) in the body of evidence for an outcome.	Lines 480-492
RESULTS			
Study selection	16a	Describe the results of the search and selection process, from the number of records identified in the search to the number of studies included in the review, ideally using a flow diagram.	PRISMA 2020 flow diagram
	16b	Cite studies that might appear to meet the inclusion criteria, but which were excluded, and explain why they were excluded.	Lines 353-355
Study characteristics	17	Cite each included study and present its characteristics.	Supplementary Figure 1
Risk of bias in studies	18	Present assessments of risk of bias for each included study.	NA
Results of individual studies	19	For all outcomes, present, for each study: (a) summary statistics for each group (where appropriate) and (b) an effect estimate and its precision (e.g. confidence/credible interval), ideally using structured tables or plots.	NA
Results of syntheses	20a	For each synthesis, briefly summarise the characteristics and risk of bias among contributing studies.	NA
	20b	Present results of all statistical syntheses conducted. If meta-analysis was done, present for each the summary estimate and its precision (e.g. confidence/credible interval) and measures of statistical heterogeneity. If comparing groups, describe the direction of the effect.	Lines 85-86
	20c	Present results of all investigations of possible causes of heterogeneity among study results.	Lines 86-100
	20d	Present results of all sensitivity analyses conducted to assess the robustness of the synthesized results.	Lines 107-109, 128-131
Reporting biases	21	Present assessments of risk of bias due to missing results (arising from reporting biases) for each synthesis assessed.	NA
Certainty of evidence	22	Present assessments of certainty (or confidence) in the body of evidence for each outcome assessed.	Lines 159-162, 176-183
DISCUSSION			
Discussion	23a	Provide a general interpretation of the results in the context of other evidence.	Lines 199-205
	23b	Discuss any limitations of the evidence included in the review.	Lines 207-223
	23c	Discuss any limitations of the review processes used.	NA
	23d	Discuss implications of the results for practice, policy, and future research.	Lines 225-257
OTHER INFORMATION			
Registration and protocol	24a	Provide registration information for the review, including register name and registration number, or state that the review was not registered.	NA
	24b	Indicate where the review protocol can be accessed, or state that a protocol was not prepared.	NA
	24c	Describe and explain any amendments to information provided at registration or in the protocol.	NA
Support	25	Describe sources of financial or non-financial support for the review, and the role of the funders or sponsors in the review.	Lines 515-517
Competing interests	26	Declare any competing interests of review authors.	Lines 523-524

PRISMA 2020 Checklist

Section and Topic	Item #	Checklist item	Location where item is reported
Availability of data, code and other materials	27	Report which of the following are publicly available and where they can be found: template data collection forms; data extracted from included studies; data used for all analyses; analytic code; any other materials used in the review.	Lines 494-513

PRISMA 2020 flow diagram for new systematic reviews which included searches of databases and registers only

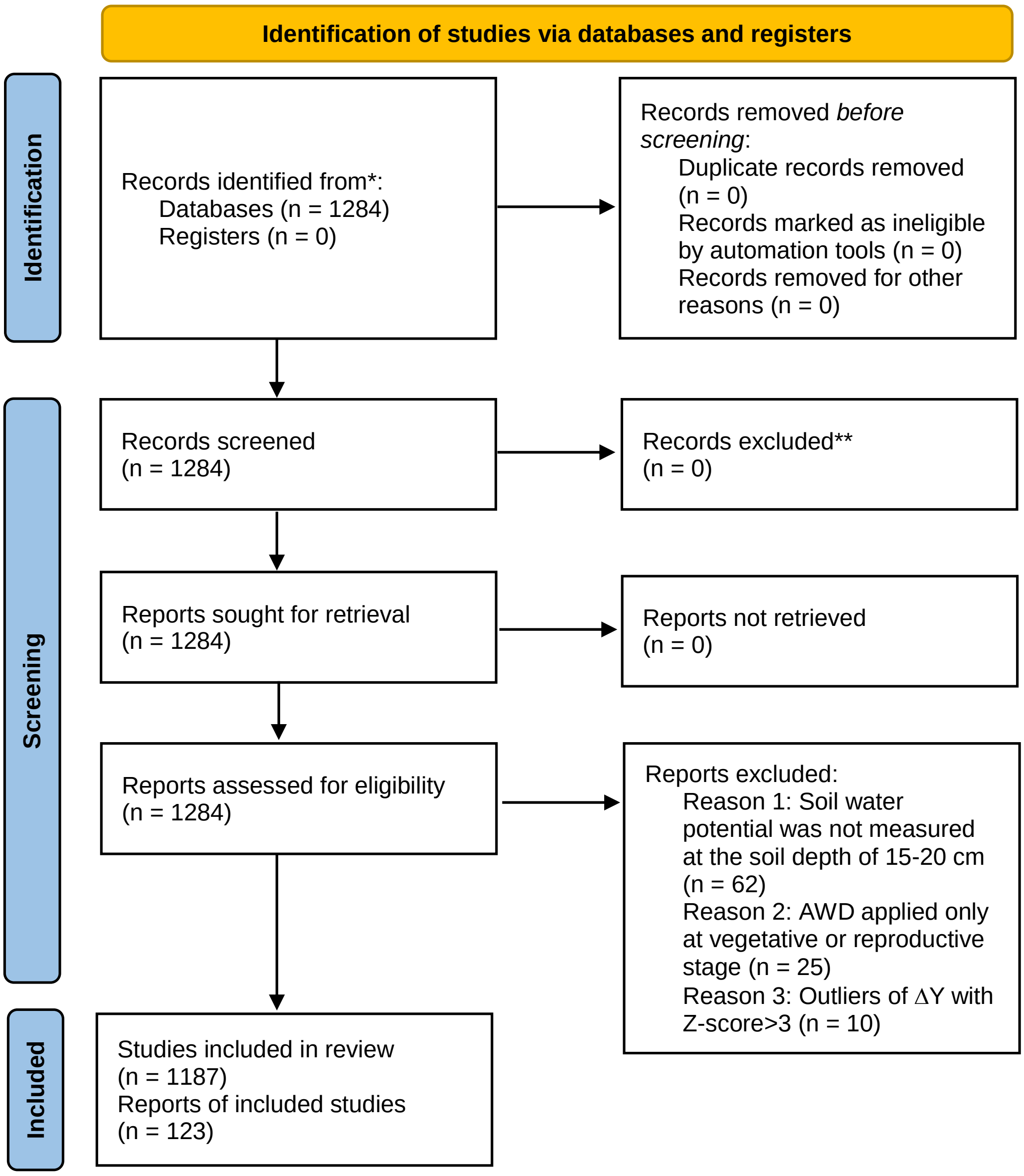

*Consider, if feasible to do so, reporting the number of records identified from each database or register searched (rather than the total number across all databases/registers).

**If automation tools were used, indicate how many records were excluded by a human and how many were excluded by automation tools.